Università degli Studi di Cagliari

DOTTORATO DI RICERCA IN SVILUPPO E SPERIMENTAZIONE DI FARMACI ANTINFETTIVI
XXVIII CICLO

"Biomimetic emulators of high potential peroxygenases: Implications in bioremediation and metabolic studies"

Sezione di Chimica Biologica
S.S.D. BIO/10

Presentata da:	Dott. Gianmarco Cocco
Coordinatore Dottorato:	Prof.sa Alessandra Pani
Tutor:	Prof. Enrico Sanjust

Esame finale anno accademico 2014 – 2015

Index

Gianmarco Cocco gratefully acknowledges Sardinia Regional Government for the financial support of her PhD scholarship, P.O.R. Sardegna F.S.E. Operational Programme of the Autonomous Region of Sardinia, European Social Fund 2007-2013-Axis IV Human Resources, Objective l.3, Line of Activity l.3.1.

ABBREVIATIONS:

AcSFP/FeTFPP *N*-Acetyl 4-Pyridyl 3-[2-(2-aminoethylamino)-ethylamino]-propyl-trimethoxysilane-fumed silica/5,10,15,20-tetrakis(pentafluorophenyl)porphine
AcSFP/FeTDCP *N*-Acetyl-4-Pyridyl-3-[2-(2-aminoethylamino)-ethylamino]-propyl trimethoxysilane-fumed silica/5,10,15,20-tetrakis(2,6-dichlorophenyl)porphine
APS Aminopropylsilica
ARS Alizarin Red S
Az A Azure A
AzB Azure B
AzC Azure C
Cpd Compound
DMSO Dimethyl sulfoxide
FeTFPP 5,10,15,20-Tetrakis(pentafluorophenyl)porphine iron(III)-chloride
HRP Horseradish peroxidase E.C. 1.11.1.7
IPS 3-(1-Imidazolyl)-propylcarbamoyl)-3-aminopropylsilica
LC Laccase E.C. 1.10.3.2
LiP Lignin peroxidase E.C. 1.11.1.14
LP Generic lignolytic peroxidase
Luperox Tert-butyl hydroperoxide
MB Methylene blue
MG Methyl Green
MO Methyl Orange
MnP Manganese peroxidase E.C. 1.11.1.13
MnTDCP 5,10,15,20-Tetrakis(4-sulfonato-phenyl)porphine manganese(III)-chloride
OXONE Potassium peroxymonosulfate
PP–PVA 4-Pyridylmethyl-3-aminopropyl-functionalized PVA, crosslinked with glutaraldehyde
PSG 4-Pyridyl-methylcarbamoyl-3-aminopropylsilica
PVA Poly(vinylalcohol)
ROS Reactive oxygen species
SFP/FeTFPP 4-Pyridyl-3-[2-(2-aminoethylamino)-ethylamino]-propyl-trimethoxysilane fumed **silica** 5,10,15,20-tetrakis(pentafluorophenyl)-porphine
SFP/FeTDCP 4–Pyridyl-3-[2-(2-aminoethylamino)-ethylamino]-propyl-trimethoxysilane fumed silica 5,10,15,20-tetrakis(2-6-dichlorophenyl)porphine
SG Silica gel
SF Fumed silica
SFP 4-Pyridyl-3-[2-(2-aminoethylamino)-ethylamino]-propyl-trimethoxysilane-fumed silica
TIO Thionine
TDCP 5,10,15,20-tetrakis(2,6-dichlorophenyl)porphine
TFPP 5,10,15,20-tetrakis(pentafluorophenyl)porphine
VP Versatile peroxidase EC 1.11.1.16
XO Xylenol Orange

List of Pubblications

- Zucca P, **Cocco G**, Pintus M, Rescigno A and Sanjust E. Biomimetic Sulfide Oxidation by the Means of Immobilized Fe(III)-5,10,15,20-tetrakis(pentafluorophenyl)porphine under mild experimental conditions. Journal of Chemistry, Volume 2013 (2013), Article ID 651274, 7 pages

- Zucca P, **Cocco G**, Manca S, Steri D and Sanjust E. Imidazole versus pyridine as ligands for metalloporphine immobilization in ligninolytic peroxidases-like biomimetic catalysts. Journal of Molecular Catalysis A: Chemical Volume 394, 15 November 2014, Pages 129–136

Abstract

Nowadays, classical (bio)remediation processes are affected by some economical and environmental drawbacks. These approaches often seem to be inadequate, particularly in the perspective of sustainable green processes. Since immobilized metalloporphines can emulate the active site of peroxidases and peroxygenases, their use in several bioremediation processes has been analyzed in this work. The described catalytic reactions use bioinspired, homogenized or heterogenized, commercial porphines and showed a remarkable ability to catalyze substrates oxidation at the expenses of different oxidants such as Oxone and hydrogen peroxide.

The biomimetic catalysts have been also investigated about their peroxidase- and peroxygenase-like catalysis and ability to emulate lignolytic peroxidases action and substrate specificity. The adducts showed a remarkable ability to catalyze veratryl alcohol (widely recognized as a simple model compound of lignin) oxidation at the expenses of H_2O_2.

In the perspective of broadening industrial applications of the described catalysts, the oxidation of several pollutants such as durable textile dyes and inorganic sulfides, has been attempted with quite promising results, and some findings open the way toward industrial scaling-up. Accordingly, the inexpensiveness of the synthesis and the mild operational conditions allow these adducts to be proposed as applicable catalysts also for industrial large-scale processes. Besides, these synthetic models are helpful also to understand the behavior of pharmaceuticals, antifungal drugs in this case, in the environment, and to predict the drug metabolism by cytochromes P450. The biomimetic catalysts, for the studied cases, also proved to be much more efficient than the corresponding enzymes.

Sommario

Oggigiorno, i processi di (bio)risanamento classici sono influenzati da alcuni inconvenienti economici e ambientali. Questi approcci sembrano essere spesso insufficienti, soprattutto in prospettiva di processi ecologicamente sostenibili. Dal momento che gli studi hanno individuato alcune metalloporfine come catalizzatori in grado di emulare il sito attivo delle perossidasi e perossigenasi, il loro impiego in diversi processi di biorisanamento è stato analizzato ed esplorato. Le reazioni catalitiche descritte utilizzano catalizzatori porfinici bioispirati, omogenei ed eterogenei, e hanno mostrato una notevole capacità di catalizzare l'ossidazione di substrati a spese di diversi ossidanti come Oxone e perossido di idrogeno. I catalizzatori biomimetici sono stati studiati per la loro capacità di emulare l'azione di perossidasi ligninolitiche e per la loro ampia specificità di substrato. Gli addotti eterogeneizzati hanno mostrato una notevole capacità di catalizzare l'ossidazione del veratril alcol, composto modello della lignina, a spese di H_2O_2. Nella prospettiva dell' aumento delle applicazioni industriali di questi catalizzatori, l'ossidazione di vari inquinanti, quali coloranti tessili e solfuri inorganici è stata studiata con prospettive promettenti e alcuni risultati sono particolarmente adatti per future applicazioni industriali. Di conseguenza, l'economicità della sintesi e le condizioni operative blande permettono a questi addotti di proporsi come catalizzatori efficaci anche per processi industriali su larga scala. Inoltre, questi modelli sintetici sono utili per comprendere il comportamento metabolico di farmaci, antimicotici in questo caso, e di prevederne le biotrasformazioni catalizzate dai citocromi P450. I catalizzatori biomimetici hanno anche dimostrato, nelle applicazioni qui descritte, di essere molto più efficienti delle loro controparti naturali alle quali sono ispirati.

1. Introduction

The increasing concern about environment contamination has led the scientific community to consider innovative methods to face pollution and to solve it with the aid of non-conventional tools such as engineered microorganisms, enzymes, and their emulators. High efficiency, effectiveness and low cost are highly desirable features for these methods to overcome the traditional physical, chemical, and biological processes [1, 2].

The main aims of the present work are to review the potential applications of the vast family of synthetic redox-active metalloporphines in the field of remediation of contaminated industrial wastewaters and to present some iconic case studies where selected metalloporphines play key roles as biomimetic oxidation catalysts [2].

Naturally occurring metalloporphines (i.e. metalloporphyrins, and in particular some heme variants) are involved as prosthetic groups of enzymes promoting reactions of bioremediation [3]; it is therefore essential to understand where they can be found, how they work and which are the determinant enzymatic systems necessary for the biodegradation process to occur. Metalloporphines are increasingly used as models of more complex systems in studies aimed at understanding the biochemical reaction pathways underlying the reactions of bioremediation.

Metalloporphines are recognized as excellent catalysts able to perform similar oxidation reactions, in several biomimetic models of enzymes such as peroxidases, heme-containing monooxygenases, and peroxygenases [4]. In this study we examine different immobilized biomimetic catalysts, which may be of interest for the oxidative degradation of different substrates [5, 6].

Biomimetic catalysts are defined as synthetic compounds that have structures somewhat resembling those of the enzyme active sites they should emulate. Usually these compounds

are therefore based on the molecular structures of prosthetic groups of the enzyme, which may be otherwise modified to improve reactivity and stability. In fact, the use of biomimetic preparations allows to obtain higher selectivity and efficiency than those achieved by conventional catalysts. They maintain meager synthesis costs, make possible a large scale production, and show a greater resistance to degradation compared to their enzyme counterparts, which require a long process of purification and often do not prove suitable for use on an industrial scale.

The ease and simplicity of bioprocess emulation control indicate significant possibilities of oxidative destruction of pollutants. The substrates to be studied and degraded arise from various industrial activities such as food production, industrial gasification processes, water treatment, tanning of hides, production and disposal of pharmaceutically active compounds and their metabolites, oil refining, textile dyeing.

In this project, biomimetic catalysts have been studied, inspired by the peroxidase enzymes, immobilized on supports of different origin, and capable of catalyzing oxidation reactions at the expense of different oxidants (hydrogen peroxide, potassium monopersulfate), and containing as their prosthetic groups suitable Mn- or Fe-porphines.

Different types of substrates were used (hydrogen sulfide, industrial dyes, veratryl alcohol, antifungal drugs) to test the versatile applications of these catalysts.

1.1 Peroxidases

Peroxidases are almost ubiquitous enzymes, usually containing ferriheme (ferriprotoporphyrin-IX) as their prosthetic group. Peroxidases could be classified into two relatively well-defined enzyme superfamilies (animal and plant enzymes, respectively) and a third rather arbitrary group that includes chloroperoxidases [7]. The plant peroxidase

superfamily is subdivided into three classes [8]: Class I includes yeast cytochrome c peroxidase and ascorbate peroxidases. Class II includes high-redox-potential peroxidases of fungal origin such as lignin, manganese, and versatile peroxidases (LIP, MnP, and VP respectively). The most prominent example of the Class III (plant) peroxidases is undoubtedly horseradish peroxidase (HRP).

Peroxidases catalyze the oxidation of a variety of molecules at the expense of hydroperoxides, most often H_2O_2. The best-studied peroxidases are monomers with MW of 30-40 kDa and contain a single, non-covalently bound heme group. Among these enzymes, those belonging to the Class II (fungal peroxidases) are by far the most interesting by an applicative perspective, being characterized by a comparatively stronger oxidizing power (high redox potential peroxidases). This feature depends exclusively on the particular 3D structure of the polypeptide chain: in fact, they contain the same usual prosthetic group ferriheme, bound to the apoenzyme by a proximal histidine residue, which forms in turn a hydrogen bond with a specific aspartate residue [9].

The peroxidase catalytic cycle can be summarized as follows:

PorphFe(III) (*resting stat*e) + H_2O_2 → PorphFe(III)–OOH (*Compound zero, Cpd 0*);

PorphFe(III)–OOH → $Porph^{+\cdot}Fe(IV)=O$ (*Compound I, Cpd I*) + OH^-;

$Porph^{+\cdot}Fe(IV)=O + e^-$ → PorphFe(IV)=O (*Compound II, Cpd II*);

$PorphFe(IV)=O + e^- + H^+$ → PorphFe(III) + OH^-.

In this scheme, Porph is the protoporphyrin IX, which binds the Fe ion and is in turn bound to the apoenzyme. *Cpd 0* is a very elusive species, rapidly evolving to *Cpd I* by a heterolytic fission of the O–O bond. It is transiently formed when hydrogen peroxide approaches the enzyme active site, where it is deprotonated by the distal histidine residue,

and the resulting hydroperoxide anion HOO^- directly binds the ferric center. The arising *Cpd 0* will therefore expel a water molecule, upon heterolytic O–O scission, directly leading to *Cpd I* [10], while the distal histidine reverts to its non-protonated form. The suggested direct intervention - if any - of *Cpd 0* as an oxidizing agent towards the enzyme substrates is still *sub judice* [11, 12] *Cpd I* is a strong oxidizing species, which could evolve through a direct oxygen donation to a nucleophilic substrate, although its one-electron reduction to the less reactive *Cpd II* is its usual fate. *Cpd I* is formed by oxidation of the catalytic site, with reduction of the hydrogen peroxide to water. With the loss of two electrons, the iron oxidizes forming a ferryl moiety Fe(IV)=O and a delocalized radical-cation in the porphyrin ring (or in an amino acid that is nearly located). This intermediate has a high redox potential and is able to oxidize, in two successive steps, two different molecules of the substrate, forming at first the *Cpd II* and then the native enzyme. Two successive one-electron steps are therefore necessary to close the catalytic cycle. It is worth noting that *Cpd II* is distinctly weaker as an oxidizing agent in comparison with *Cpd I* [13]. *Cpd 0* could in principle follow another degradation route, going through a homolytic fission of the O–O bond, and generating directly the *Cpd II,* therefore bypassing the formation of *Cpd I* and with concomitant production of the extremely aggressive $^{\cdot}OH$ radical. The hydroxyl radical could attack the substrates, or also could destroy the very ferriheme, which had generated it, therefore leading to enzyme irreversible inactivation. However, such a homolytic scission of the peroxide bond, although energetically favored, does not usually take place.

White rot fungi are typical producers of extracellular Class II peroxidases that are among their enzymatic weapons (together with laccases and other oxidoreductases) used to break lignin down [7, 10, 14-17].

Several studies have established that the fifth coordination position is occupied by an

imidazole group of a histidine residue. While, the sixth coordination position of the iron is free, in the native state, available to bind the hydrogen peroxide, during the catalytic cycle.

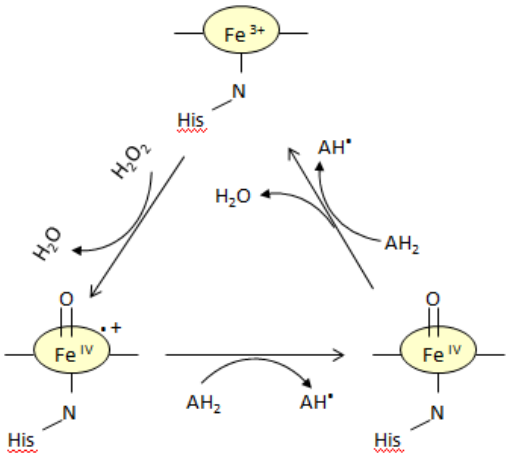

Fig. 1 A simplified scheme of peroxidase catalytic cycle

1.1.1 Lignin peroxidase

Lignin peroxidase (LiP, E.C. number 1.11.1.14) was discovered in the extracellular medium of the ligninolytic fungus *P. chrysosporium*, grown under low nitrogen availability. Since then, some other similar enzymes have been found, secreted by white rot fungi. They are monomeric hemoproteins with about 340/350 amino acids and with a

molecular mass of 40 kDa approximately; they are similar to horseradish peroxidase for containing the usual ferriheme B, coordinated with a proximal histidine.

LiPs are specialized in the oxidative demolition of lignin, at the expenses of hydrogen peroxide. The process is not completely understood and goes through a radical mechanism causing the breakdown of the C□–C□ bonds in the propanoid chains of the lignin monomeric units [18-22]. The enzyme shows a general behavior not too different from that observed in horseradish peroxidase, but its *Cpd II* is extremely labile [23] and has a sharp tendency to give the dead-end *Compound III* unless the H_2O_2 concentration is kept very low [24]. *Cpd III* (a superoxide adduct of the resting state of the enzyme) easily goes toward irreversible bleaching and inactivation. Veratryl (3,4-dimethoxybenzyl) alcohol, which is a secreted metabolite of *P. chrysosporium* [25], shows a protective action towards the enzyme. It is moreover a natural mediator, playing a key role in breakdown of lignin fragments, exceeding 20 monomeric units.

$$\mathbf{LiP(Fe^{3+})P + H_2O_2 \rightarrow LiP\text{-}I(Fe^{4+}\text{-}O)P^{\bullet} + H_2O}$$

$$\mathbf{LiP\text{-}I(Fe^{4+}\text{-}O)P^{\bullet} + R \rightarrow LiP\text{-}II(Fe^{4+}\text{-}O)P + R^{\bullet}}$$

$$\mathbf{LiP\text{-}II(Fe^{4+}\text{-}O)P + R + 2H^{+} \rightarrow LIP(Fe^{3+})P + R^{\bullet} + H_2O}$$

The outstanding functional difference between LiPs and ‘classical’ (Class III) peroxidases is that LiP can oxidize aromatic rings that are only moderately activated by electron-donating substituents, while classical peroxidases act only on strongly activated aromatic substrates. Thus LiP and HRP oxidize both 1,2,4,5-tetramethoxybenzene, phenols and anilines, but only LiPs are capable of drawing one electron from moderately

activated aromatic compounds such as veratryl alcohol. The arising radical cations obtained could evolve via proton expulsion or via nucleophilic attack (usually by water), and therefore complex mixtures of different oxidation products are found [26-28].

LiPs present a tryptophan residue (Trp 171 in *P. chrysosporium*) which participates in long distance electron transfer from bulky substrates to the ferryl center of the enzyme [29]. This tryptophan residue is β-hydroxylated as a result of enzyme activity. More polar, small substrates are oxidized at the exposed heme edge [23].

1.1.2 Manganese peroxidase

Manganese peroxidase (MnP, E.C. number 1.11.1.13) is an enzyme, common among white rot fungi, and very similar to the previous one, but with different substrate specificity: in fact, it is able to oxidize Mn^{2+} (present in traces in the wood) to Mn(III) complexes (the Mn^{3+} ion cannot exist as such in aqueous solution). The latter act as oxidizers towards lignin, with a radical mechanism, and the arising manganous ion is retaken back into the catalytic cycle [30]. MnP active site lacks the above mentioned tryptophan residue, and shows instead a negatively charged cluster needed to complex the Mn(III) species arising from the enzyme activity [27]. The enzyme is typical for the very low oxidizing power of its *Cpd II*, which compulsorily requires Mn^{2+} to be reduced to the enzyme resting state [31, 32]. The enzyme is not able to oxidize the non-phenolic lignin units, as it lacks the key tryptophan residue needed for the long distance electron transfer from the substrate to the ferryl center; however it can oxidize the phenolic units. Anyway, phenolic units are only of secondary importance in lignin structure, and therefore this ability has only a limited influence towards lignin fragmentation and solubilization.

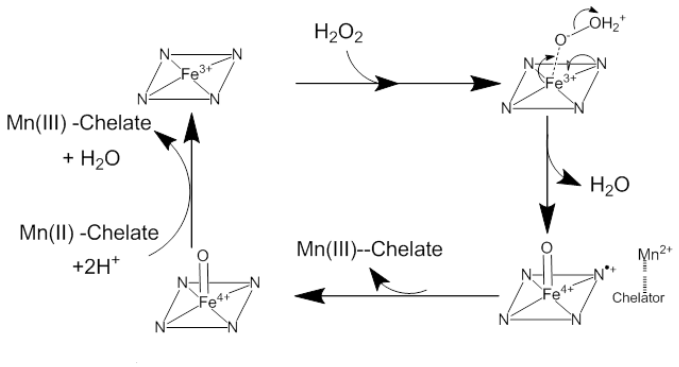

Fig 2.Catalytic mechanism of MnP.

The electron-donating power of anionic chelators, such as oxalate, increases the electron density on the Mn(III), making it a weaker oxidant. However, it is still capable of slowly oxidizing the numerous non-phenolic lignin structures. Mn(III) chelates can easily attack the phenolic structure of lignin, but the oxidation of these units does not result in an increased lignin degradation.

1.1.3. Versatile peroxidase

Versatile peroxidases (VPs) seem to be a sort of 'hybrid' enzymes between LiPs and MnPs, as they bear both the key tryptophan residue of LiPs and the anionic cluster of MnPs [33]. By consequence, they show wide substrate specificity, and could be the 'ideal' enzymes for lignocellulosics biodegradation. However, a typical VP producer, the white rot fungus *Pleurotus eryngii,* is a poorly effective lignin degradator.

Delignification of wood pulp using redox enzymes is considered an alternative to chemical bleaching. It has the substantial advantage of requiring low pressures and temperatures, and on the whole quite mild operative conditions. However, the required enzymes are usually rather costly, and moreover both LiP and MnP are very sensitive to irreversible bleaching and inactivation upon treatment with even a slight excess of peroxide. Nevertheless, in principle such peroxidases (and peroxygenases) have great

potential not only in wood biopulping, but also in the bioremediation of industrial dyes present in the print waste products and textile industry.

1.2 Peroxygenase

A relatively 'new' class of hemoenzymes involved in ligninolysis and typical for its unusual wide substrate specificity is that of peroxygenases (E.C. 1.11.2.1). Fungal peroxygenases have been thoroughly studied by Hofrichter and colleagues [34-39]; these enzymes are extracellular hemoproteins secreted by a few ligninolytic fungi and clearly related to cytochrome P450 family, for having a thiolate ion of a specific cysteine residue as the fifth coordinating ligand instead of the proximal histidine imidazole found in LiP and MnP. Peroxygenases are a kind of 'hybrid' enzymes between peroxidases and cytochromes P450: by reaction with hydroperoxides they form - therefore paralleling peroxidases - the corresponding *Cpd I*; this latter has a sharp tendency to act as a monooxygenating species in a way quite resembling that of the well known heme-containing monooxygenases. Peroxygenases monooxygenate (hydroxylate or epoxidize) benzylic carbons, phenyl rings, and even inert heterocycles such as pyridine. show wide substrate specificity, being able to use hydrogen peroxide to oxygenate (epoxidize and/or hydroxylate) aromatic rings benzylic carbons, and even recalcitrant heterocycles such as pyridine. They can also behave as bromide peroxidases (but, somewhat surprisingly, not as chloroperoxidases). Their unique action mechanism and substrate (wide) specificity makes these enzymes of the highest potential interest as bioremediation tools. The disadvantage of using hydrogen peroxide (instead of the cheapest amongst oxidants, i.e.

air oxygen, with is the 'normal' oxidant for cytochromes P450), is largely compensated by the fact that no any external reductant is need (whereas cytochromes P450 compulsorily require the very expensive NAD(P)H.

1.3 Redox-active metalloporphines. Biomimesis, bioemulation, bioinspiration

Porphyrins are a class of natural macrocyclic compounds, which play a key role in the metabolism of nearly all forms of life.

Although usually indicated as porphyrins along the literature, almost all the synthetic compounds usually referred to as such should be more correctly indicated as porphines, according to IUPAC nomenclature instructions. As a rule, the macrocycle, whose eight peripheral (or β) positions do not bear any organic substituent, is a porphine that could conversely bear substituents at the four methine bridges (the *meso* positions). It is worth noting that the natural porphyrins always bear eight organic substituents at their β positions, whereas the *meso* positions are invariably free. In conclusion, porphyrins are porphines, whose eight peripheral positions all bear organic substituents.

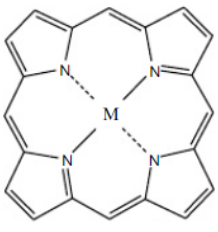

Fig. 3 Generic metal complex of the fundamental macrocycle porphine

The porphine nucleus is a ligand, where the space available for a metal ion has a maximum diameter of about 3.7 Å. When there is the coordination, the two internal protons are removed, leaving two negative charges. The system of rings of porphines and porphyrins shows an aromatic character, according to the Hückel rule. Porphines and porphyrins easily form stable complexes with all metallic or semimetallic elements [40].

Some porphyrin metal complexes play important roles in biological systems, ferroheme and ferriheme being the commonest and outstanding examples. Among other macrocycles, more or less similar to true porphyrins, chlorophylls and corrinoids can be mentioned.

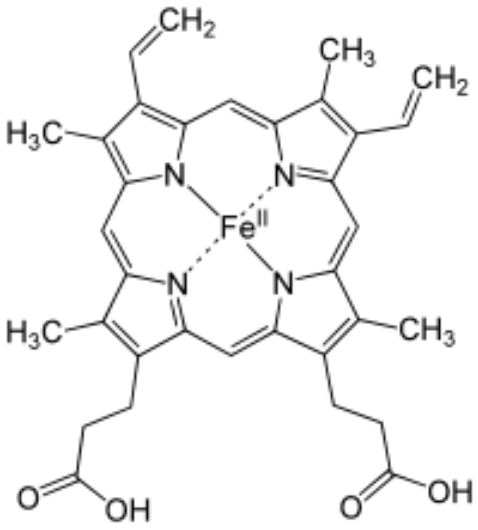

Fig. 4 Structure of the ferrous complex of the iconic protoporhyrin IX (ferroheme).

Porphyrin and porphine chemistry is rather complex, and is strongly influenced by the metal ions, which could be complexed at the center of the macrocycle. The most studied

complexes are those formed with Fe(III) and Mn(III) and, up to a minor extent, with Ru(III). It is important to note that many oxidation numbers, assigned to the central metal ions in metalloporphines, have a largely *formal* value due to tendency of the macrocycle to accept some electronic density from the metal ion into its π* (antibonding) orbitals. Although many metalloporphyrins and metalloporphines show photocatalytic activities, their most interesting feature is the ability of catalyzing redox reactions, usually involving O_2, H_2O_2, ClO^- and a number of other oxidizing agents acting as single oxygen atom donors [40]. Such redox activities are as a rule connected to the presence of a redox-active ion (such as those deriving form Fe, Co, Mn, Ru, Cu, V, Cr and so on) within the center of the macrocycle. Some important differences have to be underlined when considering the catalytic activities of heme-containing peroxidases, peroxygenases, and monooxygenases on one hand, and free metalloporphines on the other one. In fact, the apoenzymes play a crucial role in modulating the chemical features of the metalloporphyrins, buried within the polypeptide scaffolds. First, the protein exerts a rather efficient protective action towards the metalloporphyrins, which would be otherwise rapidly bleached and destroyed by the oxidizing agent. Second, the axial coordination by a specific histidine (peroxidases) or cysteine (peroxygenases and monooxygenases) residues deeply influences the general and specific reactivity of the holoenzyme. Substrate access to the active site is moreover determined by the particular primary, secondary, and tertiary structure of the polypeptide chain surrounding the metalloporphyrin [41].

Free metalloporphines are not subjected to the restrictions imposed by any apoenzyme, so their reactivity mainly depends on their particular structures, i.e. *meso* and β substituents, and on the nature of the metal ion. The most obvious consequence is a substantial lack of specificity in their catalytic action, being their surface (that of the

'sixth' coordination site) well exposed to the solvent. This extreme versatility of the redox-active metalloporphines (both on the side of the substrate specificity and on that of the action mechanisms) could be a serious drawback when envisaging the use of such catalysts for synthetic purposes [6]. On the other hand, it is a very valuable feature when the preparations have to be used for remediation purposes, but is weakened by an unwanted, pronounced sensitivity to bleaching by the oxidizing agents used along the remediation process. Nowadays, a wide variety of synthetic metalloporphines have been synthesized, and many of them are commercially available at reasonable prices. The common target of the studies dealing with redox-active metalloporphines is to combine chemical robustness with high catalytic efficiency, to overcome the limits observed in natural metalloporphyrins such as ferriheme (hemin). Along the years, the chemical structures of synthetic metalloporphines were gradually improved: initially, the *meso*-tetraphenylporphine was shown to be a substantial progress when compared to hemin, being more stable in spite of its poor catalytic efficiency. A further step forward [42, 43] was made when introducing electron-withdrawing substituents on to the *meso*-phenyl rings, and/or bulky substituents in the *ortho*-positions of the same rings, to prevent coplanarity with the porphine macrocycle. Alternatively, phenyl rings can be replaced by N-methylpyridinium rings [44]. By this way, a substantial improvement of both stability and activity was achieved. Another improvement was accomplished by substituting some or all the hydrogen atoms at the β positions with strongly electron-withdrawing moieties, such as nitro or sulfonic groups, or halogens such as bromine, chlorine, or fluorine. However, the β substitutions have sometimes produced contradictory results, and in particular bromine atoms are bulky enough to hinder substrate approach to the oxidized metal center within the porphine ring. On the contrary, perfluoro substitution gives rise to rather costly but exceptionally robust and active catalysts [45]. Avoiding coplanarity is in

general very important to prevent undesired substituent activation at the para position of the phenyl moieties, as observed by Kadish and colleagues [46] in the case of TFPP: fluorine atoms on the four *meso*-phenyls are not bulky enough to avoid coplanarity. Metalloporphines are quite hydrophobic and therefore almost insoluble in water, unless sharply hydrophilic substituents are inserted in their structures such as the above-mentioned sulfonate or N-methylpyridinium groups. When such substituents bear net electric charges, an additional advantage is the mutual electrostatic repulsion, which prevents stacking or aggregation [47, 48].

Many redox-active metalloporphines easily react with oxygen donors such as hydroperoxides and peroxyacids, thus affording high-valent oxo derivatives [49-51], similar to those found along the catalytic cycles of peroxidases, peroxygenases, and heme-containing monooxygenases belonging to the P-450 family: the *Cpd I*. While peroxidases are usually incapable of performing oxygen transfer reactions (the redox reactions with oxidizable substrates take place at the heme edge [52]), the things go differently for monooxygenases and peroxygenases, where the substrate molecules could easily approach the high-valent iron center. It is also worth noting that the ability of these enzymes to perform oxygen transfers to substrates seems to be related to the substitution of the proximal histidine residue with a cysteine. Emulation of both P450 enzymes and the less studied peroxygenases has been and is the focus of much attention, since monooxygenation and epoxidation reactions are of high synthetic relevance. The structures and properties of the *Cpd I* and *II*, pertaining to P450 enzyme family, are discussed in a review [53] . P450 enzymes compulsorily require NAD(P)H as a co-reductant of molecular oxygen they use to monooxygenate a wide variety of substrates [54], so their importance in biotechnological applications is limited. Owing to the absence of any protein protective scaffold, redox active metalloporphines could follow

different catalytic pathways, depending on their own molecular structures, on the central metal ion, on the substrate to be oxidized, on the experimental/operative conditions [55]. The observed mechanisms could therefore go through a direct (or also indirect, oxygen rebound mechanism transfer [56]), or through mono-electronic oxidations.

In principle, all these mechanisms could work at the same time.

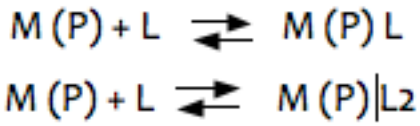

Simple metalloporphines and metalloporphyrins present as a rule a square planar coordination of the central metal ion, although this geometry can be more or less profoundly distorted when a bulky metal ion is involved that cannot fit perfectly to the central place within the porphine macrocycle. However, the vast majority of redox-active metal ions prefer a higher coordination number, namely 6, so four equatorial and two axial coordination bonds are observed in the presence of proper ligands, leading to an octahedral geometry. The axial ligands deeply influence the chemical behavior of the resulting complex, included the reactivity towards molecular oxygen and other oxidants [57]. The high tendency of the central metal ion to expand its coordination sphere therefore ligating at least an axial species (such as in deoxy myoglobin and hemoglobin, or in the resting state of the peroxidases) or also two, identical or different (such as in many cytochrome families) is shared among physiologically relevant metalloporphyrins and synthetic metalloporphines, and is of crucial importance to tune the reactivity of the resulting complexes and to determine their potential applications. It was noted that too

affine ligands shift the balance in favor of the hexacoordinate complex, making the interaction of the metal ion with molecular oxygen or other oxidants difficult, or very often physically impossible. In conclusion, too feeble interaction is of poor significance and therefore useless in the view of stabilizing the metalloporphine and/or increasing its catalytic activity. On the other hand, too affine ligands prevent any reaction but simple electron exchanges (as those observed in many cytochromes). Moreover, the axial ligand must be capable of binding the metal in its higher oxidation states, without making the intermediates too stable thus preventing the next reaction, that is the oxygen transfer to the substrate (or the electron exchanges) and the reduction of the intermediate to restore the native catalyst [57]. The stabilizing and activating effect of suitable ligands for the axial position has been by far recognized, and imidazole has been often described as an important component of the reaction mixtures conceived to optimize metalloporphine catalysis.

Biomimesis consists, according to the well-known definition of Breslow, in the design, synthesis and study of artificial systems to mimic, in a simple way, some aspects of the operation of the equivalent biological systems. This is just the case of the use of imidazole added as a stabilizer and a catalytic enhancer for redox-active metalloporphines.

Generally speaking, when the biological systems of interest are enzymes, enzyme models could be conceived and often constructed. This approach, which uses less complex systems than the natural ones and therefore more suitable for detailed studies, presents the double utility of allowing, from one side the verification of mechanistic hypotheses and the study of the parameters influencing the action mechanisms of biological systems and, on the other, the discovery and development of new compounds able to perform new functions.

“Enzyme models” are proposed to reproduce one or more of the outstanding features of natural enzymes. The most effective approach in the realization of biomimetic systems is gradual and cannot be separated from the study of the structure and mechanism of action of enzymes that have to be emulated [1].

Synthetic metalloporphines can behave as biomimetic catalysts that emulate the catalytic activity of peroxidases and peroxygenases, because they can perform efficient oxidation and degradation of an incredible variety of organic molecules, ranging from lignocellulosics to polycyclic aromatic hydrocarbons to industrial dyes [2, 5, 58].

Properly functionalized metalloporphines, bearing suitable substituents in their *meso* positions, are very stable catalysts towards oxidants; their redox potentials and their solubility can be finely adjusted by the features of the substituents.

Some significant differences have been found when comparing Fe-porphines to Mn-porphines. In particular, Mn-porphines form a relatively stable, although highly reactive, oxidizing species, *Cpd I* analog, where the oxidation state of manganese is +5. This implies that no a π radical cation is formed at the expenses of the porphine nucleus, and a porphMn(V)=O structure can be assumed for these catalysts. As a consequence, Mn-porphines show a noticeable tendency to catalyze oxygen transfer reactions (peroxygenase-like) when compared to their Fe-containing counterparts, more prone to participate in peroxidase-like reactions.

1.4 Immobilization

Generally speaking, the use of a catalyst for process applications requires its reuse and recovery at the end of the process. These properties may not be present in a catalyst used in soluble form because its separation from unchanged substrates and formed products is

usually a quite hard task. Only in selected cases a soluble catalyst could be discarded, provided that it is harmless, its presence will not jeopardize the subsequent purification of the product, and its cost is decidedly low. Soluble catalysts only seldom meet these conditions, and this is the main reason why soluble catalyst are immobilized whenever possible. Immobilization usually implies heterogenization (the obtained preparations are insoluble in the reaction medium), which allows facile recovery of the catalyst and its repeated reuse by simple physical operations such as decantation. Immobilization as a rule lowers catalyst efficiency (mainly due to diffusion issues) but on the other hand enhances its stability. The metalloporphines who work free in solution, in the presence of hydrogen peroxide, may promote the desired oxidation reaction, or undergo side reactions, such as the homolytic cleavage of the O–O peroxide bond, with release of hydroxyl radicals as noted above. Moreover, a secondary catalase-like activity leading to peroxide dismutation and wasting could be observed.

Another undesired reaction is dimerization of the metalloporphines *via* an oxo bridge between the two metal ions. This phenomenon is particularly favored for uncharged, hydrophobic metalloporphines, that easily undergo stacking and aggregation. In the 70s of previous century, some researchers circumvented these problems by tying the catalysts on solid supports, by exploiting techniques already well known in the field of immobilized enzymes. During the past decades, research has devoted considerable time to produce immobilized catalysts on a large scale. Different supports, such as synthetic organic polymers, biopolymers or inorganic materials, were used. Several approaches were explored, taking advantage of different types of catalyst-support linkages, such as ionic, covalent, coordination or adsorption or entrapment in the pores of solid matrices.

The purpose of immobilization is to balance the loss of initial activity, preserving it for a long time. In general, the continuous activity is more valuable than the initial activity. The

adsorption is probably the simplest technique, but often not profitable because the bonding forces between the catalyst and the carrier may be weak, so that the catalyst can be easily desorbed along the catalytic process. On the contrary, the physical entrapment in polymeric gels or membranes prevents the leaking of the catalyst, allowing the passage of substrate and products. However, this technique implies the careful preparation of 3D polymeric networks or hollow spheres, beads, or fibers: the consequence is a sharp increase in costs.

In this study, the chosen metalloporphines have been immobilized on conventional solid supports: silica gel and polyvinyl alcohol, whereas fumed silica was used for the first time ever; in fact, after extensive research testing different matrices, fumed silica has been identified as a new, very promising candidate for the development of new supports for immobilized metalloporphines.

The use of strongly polar and hydrophilic supports allows the preparation of fully water-compatible heterogenized catalysts also starting from quite hydrophobic metalloporphines.

Silica gel is one of the most interesting inorganic supports [1], because it is non-toxic, physically and chemically robust, easily available in huge amounts, quite inexpensive. Silica gel is usually produced starting from *ortho*-silicic acid (H_4SiO_4) by gradual dehydration and condensation under controlled conditions; it is composed by a compact 3D network of siloxane groups Si–O–Si within the structure and by silanol groups, Si–OH, distributed on the surface.

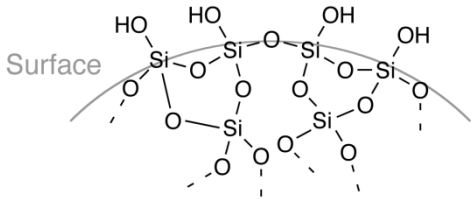

Fig. 5 Schematic Surface Of Silica Gel.

The silica matrices so obtained possess amorphous structures, similar to that of glass. The silica gel surfaces are strongly polar, owing to the presence of several silanol groups; these are slightly acidic and show a sharp tendency to form strong hydrogen bonds; the presence of so much silanols allow the silica to fix more or less firmly polar substances that come in contact with it [1]. In other words silica gels show high adsorptive properties towards a huge variety of chemical species; this is a desirable feature when chemisorption is a way to adsorb chemicals from their solutions, whereas is a drawback for its lack of specificity.

Differently for common silica gels, fumed silica (not to be confused with silica fume [59]) is obtained by burning $SiCl_4$ at high temperatures, injecting the reagent within a flame. The cooling of fused silica droplets out of the flame is so rapid that they cannot crystallize and form instead a glassy material. The primary droplets (size ranging between 5 and 50 nm approximately) aggregate to form branched chains, which in turn can form new 3D superstructures. Fumed silica is non-porous, but the very small size of the primary particles ensures a very high surface area (ranging from 50 to 600 m^2/g approximately) This method of preparation is responsible for the comparatively high reactivity of the surface, which is also very hygroscopic, provided that the bond tensions of the surface Si–O–Si motifs are resolved upon hydration. The most outstanding feature of fumed silica is its exceptionally high surface/volume ratio. Even fumed silica is composed of internal siloxane groups Si–O–Si, and a few silanol Si–OH groups on the surface; the surface density of such silanols groups dramatically rises upon hydration; the presence of these latter confers the silica its strong adsorptive properties .

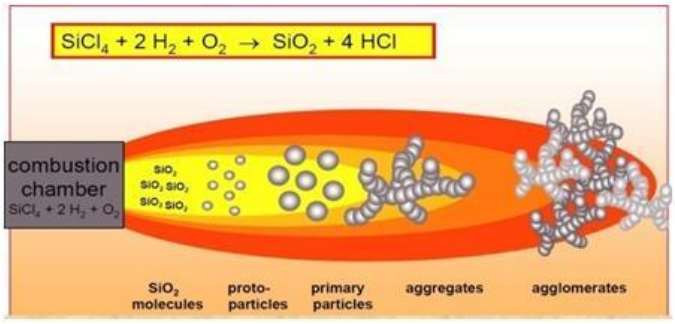

Fig.6 Preparation of Fumed Silica in Flame

Fumed silica has been used as a very effective adsorbent for a wide range of compounds, and also for proteins and enzymes [60-63].

Fumed silica is also especially reactive owing to its high surface/volume ratio: in the present study, its functionalization with the conventional techniques (i.e. silanization) is described in detail.

This kind of silica is used for the first time in this study as a support for the immobilization of metalloporphines.

PVA is an inexpensive, non-toxic, biodegradable, hydrophilic, water-soluble polymer, suitable for a wide range of modification reactions including crosslinking and therefore of potential interest for a number of applications, including enzyme immobilization and topochemical functionalization [58]. In the present study a crosslinked and functionalized structure was obtained by acetalation with suitable aldehydes under strong acidic conditions. A transparent, colorless, highly hydrophilic but totally insoluble gel was obtained, capable of specifically bind metalloporphines.

1.5 Industrial Dyes

Dyes are chemical compounds characterized by absorbing in the visible region of the electromagnetic spectrum (400 to 700 nm). Until few years ago, most of the dyes come from natural sources such as leaves, roots and berries (upon maceration), or were mineral compounds.

In the late nineteenth century William Henry Perkin worked to the synthesis of quinine, a plant alkaloid used in the treatment of malaria. He tried to synthesize quinine by the oxidation of aromatic amines and he prepared, instead, precipitates of strong purple color. This dye was named Mauveine, proved to be an excellent dye for tissues and become the first synthetic dye. Since then, the development of the synthetic dyes began. Their application over the different affined substrates (textile materials, leather, paper, hair, etc.) is performed from a liquid in which they are completely or partially soluble [64].

The synthetic dyes represent a large group of organic compounds that could have undesirable effects on the environment, and in addition, some of them can pose risks to humans [65-67]. They are very often recalcitrant compounds and become dangerous pollutants when released in groundwater. By definition, an industrially applicable dye should be a quite resistant compound, capable of surviving against harsh conditions such as prolonged exposition to sunlight, and harsh washing and/or bleaching treatments. Accordingly, they are very often recalcitrant with respect to chemical and biological degradation processes [68-71].

Unfortunately, the demand has led nowadays to the widespread use of synthetic colors. They represent the most economical solution for industries, both for the higher performances compared to the natural ones, both for considerably lower costs.

The synthetic dyes have the characteristic of being absorbed by the fabrics (affinity) and to stay fixed (solidity).

In a dye molecules two main moieties can be noticed: chromophore and auxochrome. The chromophore is the group responsible for the color; the auxochrome is the group that intensifies the color [64]. Other chemically varying groups are responsible for dye solubility in proper solvents (generally water for textile dyes) and for fixation on to the fabrics.

From the point of view of the chemical structure, taking into account the dye classes that have been subject of degradation studies implying the use of metalloporphine-based catalysts, dyes can be classified according to the chromophores present in their molecules, as follows:

1.5.1 Azo Dyes.

These synthetic dyes are typical for the presence of one or more chromophoric groups –N=N–. Commercially, azo dyes represent the most important class of synthetic dyes, as they show at the same time facile production at low cost, bright colors with a number of beautiful different nuances, high affinity and solidity. The double bond N=N, placed between the two aromatic portions, is called azo group and it is a strong chromophore conferring a bright color, usually ranging from yellow to orange to red [72]. Very often, one of the two aromatic moieties is electron-withdrawing (it may contain, nitro and/or sulfonate groups, or so on) whereas the other one is electron-rich (it usually contain electron-releasing groups such as hydroxy, amino, dialkylamino, and so on). An example of an azo dye is the Methyl Orange, used for dyeing wool and silk.

As a general feature, azo dyes are toxic to many forms of life. Many have been withdrawn – in particular among those used for dyeing food – because of their

carcinogenic properties. Their toxicity arises from their *in vivo* reduction to aromatic amines by an enzymatic cleavage of the azo group [65]. Therefore, their massive presence in wastewaters, released by textile plants, represents a major concern in the perspective of solving the severe pollution problems caused by such plants.

1.5.2 Anthraquinone dyes.

These derive from the almost colorless 9,10-anthraquinone. The industrially relevant derivatives contain powerful electron-donating groups as auxochromes, such as amino or hydroxy substituents, in at least one of four alpha positions. Some hydroxyanthraquinones are of natural origin but could be industrially synthesized with sharply lower costs, whereas many others (amino-, nitro-, and/or sulfo-derivatives) are synthetic. Simple anthraquinone dyes include Alizarin (1,2-dihydroxyanthraquinone), once obtained by *Rubia tinctorum*, and its non-natural derivative Alizarin Red S (1,2-dihydroxyanthraquinone-3-sulfonic acid).

The anthraquinone dyes are among the most durable industrial dyes and therefore are used when high resistance against sunlight and/or harsh environmental conditions is required. Such a feature could be a significant problem for their degradation [5].

1.5.4 Cationic dyes.

Cationic dyes [73] should be defined as dyes, whose positive charge(s) are essential part of their chromophores. They should not be confused with other dyes, whose positive charges are not involved in the chromophoric structures, but have the main function of conferring solubility in water and/or the ability of forming strong ionic interaction with negatively charged fibers. Several applications have been described for these dyes [74, 75]. Many *stricto sensu* cationic dyes belong to the cyanine group (in turn a subclass of the

polymethine family), showing a variable number of conjugated double bonds ending with two nitrogen atoms at the two termini of the unsaturated chain. The odd number of carbon atoms forming the unsaturated chain implies the presence of a net positive charge, delocalized between the two terminal nitrogen atoms. Many dyes belong to the group, although many are conventionally classified as diphenylmethane, triphenylmethane, fuchsoneimine and benzophenoneimine derivatives, and moreover their condensed and/or internally bridged derivatives [76, 77]. Being on the whole electrophilic species, such dyes are usually rather resistant against oxidation, unless they are changed into the corresponding pseudobases, at high pH values.

1.5.5 Azine dyes.

These deserve a special mention because a particular series (thiazines) has been studied in the present work. A generic azine is defined as a heterocycle, formally derived from benzene, where one or more =CH– groups are substituted with nitrogen atom(s) =N–. Azine dyes are formally derived from pyrazine (1,4-diazine), or from its isologs oxazine (1,4-oxazine) and thiazine (1,4-thiazine). In fact, to have a dye, the fundamental heterocycle has to be ortho-condensed with two benzene rings, in turn bearing suitable substituents. The mother sulfur compound is known as phenothiazine, whose simplest dye derivative is thionine, 3,7-phenothiazinium (usually found as the acetate).

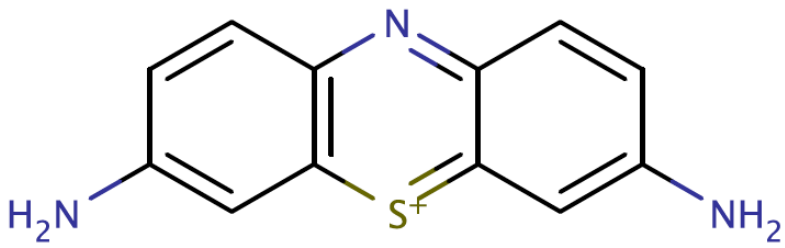

Fig. 7 Thionine structure

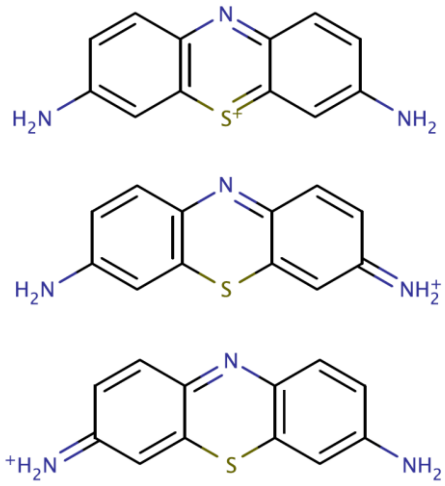

Fig. 8 Resonance structures of Thionine.

The violet dye bears a net positive charge, largely delocalized among the sulfur atom and the two amine groups, so the molecule is on the whole electrophilic in character. However, all the heteroatoms host non-bonding (lone) electron pairs, which could in principle act as nucleophiles towards an oxidant, strong enough to start a redox reaction going through a radical mechanism. The figures below show some of the mesomeric structures of thionine,

meaning that the same type of relocation occurs also for the derivatives methylated at the level of amino groups. Thionine (is available commercially as acetate).

Methylated thionine derivatives:

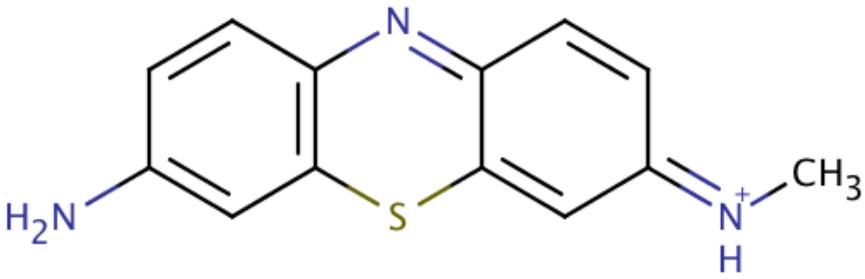

Azure C (monomethylthionine.) Fig. 9

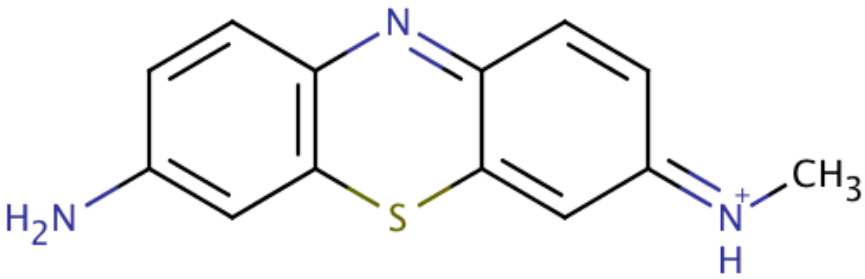

Azure A (N,N-Dimethylthionine) Fig. 10

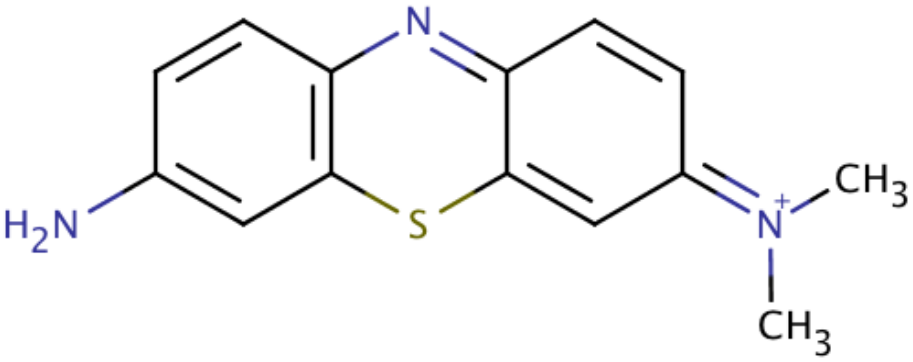

Azure B (Trimethylthionine). Fig.11

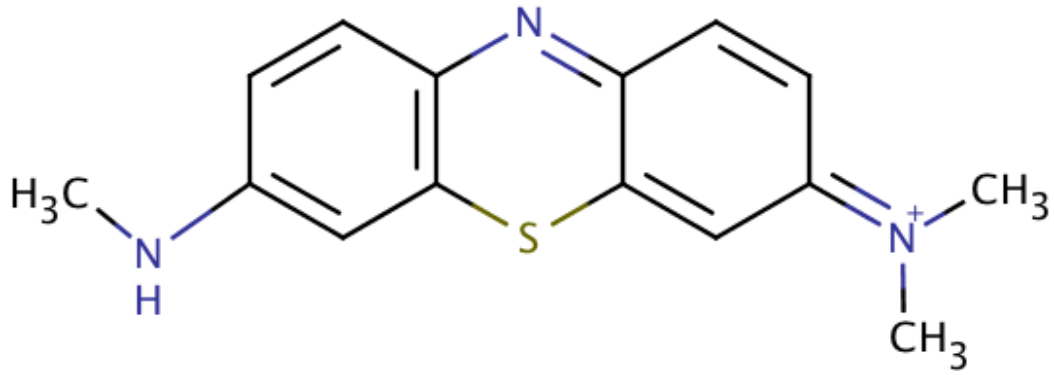

One of the most important is certainly the thiazine dye methylene blue: this dye is used in various fields, including biology, chemistry and medicine, therefore dangerous for both the environment and the human health [2, 78].

Methylene Blue (3,7-bis(Dimethylamino)-phenothiazinium) Fig. 12

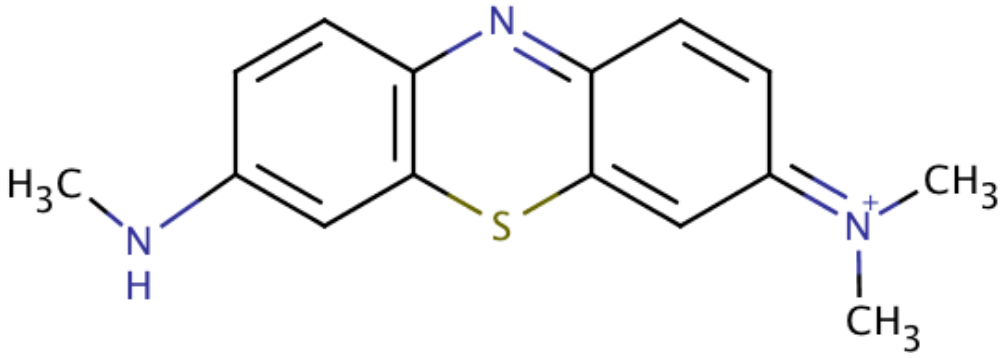

The methyl substituents present in Thionine dyes are weak donors of electron density and so favor the jumping of the π electrons from the fundamental state to the excited one (bathochromic effect). The lower energy difference between a level and the other, means that less energy will be necessary to make the electronic jump. Therefore the bathochromic

effects become more and more evident with increasing the number of methyl substituents. An important difference between Methylene Blue and other thiazines consists in the fact that Methylene Blue cannot be deprotonated, being a quaternary immonium salt: it is a decidedly stronger base in comparison with not fully methylated thionines, and retains its net positive charge also at relatively high pH values were the less methylated thionines exist - at least in part - as uncharged quinoneimines.

1.6 Sulfides and H_2S

Hydrogen sulfide is a colorless gas, typical for being a potent stench, with a very bad smell of rotten eggs. It is a very toxic compound, responsible for industrial poisoning or death, although its very low olfactory threshold could effectively warn the exposed personnel. Hydrogen sulfide is slightly soluble in water, where it behaves as a weak acid, and is then named hydrosulfuric or sulfhydric acid. H_2S Forms insoluble salts with heavy metals, whereas alkaline and ammonium sulfides are very soluble in water. It occurs naturally in oil or gas fields, and is obtained as an undesired byproduct through desulfurization of coal and in preparation of syngas. It is also contained in some volcanic emanations, where is formed by the action of steam on sulfides; in mineral waters, where it arises by bacterial reduction process of sulfates. In fact, emissions containing hydrogen sulfide are a health and environmental issue [79]. Monoalkyl or aryl derivatives of H_2S show the formula R–SH and are known as mercaptans or thiols; the disubstituted derivatives R_2S are the organic sulfides. Either H_2S and its organic derivatives are readily oxidized; in any case, only H_2S has a strong tendency to produce colloidal sulfur, whose recovery from the suspensions is particularly arduous, while thiols and organic sulfides are oxidized to the relatively harmless and sharply hydrophilic sulfonic acid and sulfones, respectively.

Several methods have been proposed for its degradation, chemical and physical processes [80, 81]. However, usually they are characterized by extreme operating conditions, transforming the entire process in an operation economically impactful.

Furthermore, microbiological methods have been recommended, showing however some drawbacks concerning the long time of reaction, stability, and compatibility of the rubbery membranes with the gas components [82, 83].

Still an enzymatic alternative has been described [84, 85], since organic sulfides (thioethers, R–S–R) can be selectively oxidized to the corresponding sulfoxides and sulfones under very mild conditions with the help, for example, of BDS (biodesulfurization) [85, 86] catalyzed by enzymes such as oxygenases; but the industrial applicability of enzymatic BDS has not yet been obtained, since the enzyme sources are limited and the costs are too high [84].

Not perforce BDS conducts to sulfur elimination from sulfur-containing organic molecules. In many cases, thiols and thioethers, respectively, mutate to sulfonic acid and sulfones. An other approach to eliminate thiols has been suggested, involving the synergy of mushroom tyrosinase, air, and suitable catechols. The o-quinones arising from the enzyme action covalently bind thiols affording nearly odorless compounds [87].

1.7 Lignocellulosic materials

Every vegetable material containing biopolymers as three main components: cellulose, hemicellulose and lignin, can be defined as lignocellulosics. This category includes agricultural wastes such as straw, pruning, seeds, fruit and vegetable peels, pits, hulls, shells, leaves, and wastes of the forest and paper industry, such as wood waste, leaves, bark, sawdust, shavings, fiber rejects, etc. These are materials that have multiple uses (paper production, natural and synthetic fibers) and represent approximately 50% of the world's

biomass, with an estimated annual production of around one hundred billion tons.

Fengel and Wegener [88] estimate the presence of 2.5–4x10^{11} tons of cellulose and 2–3x10^{11} tons of lignins in earth, that correspond about to 40% and 30% of total organic matter carbon.

The lignocellulosic materials are biodegradable substances, but often have very long half-lives, even some centuries, depending on the origin and composition.

The lignocellulosic fibers are plant cells that have evolved to allow the transport of water and solutes across the entire body of the plant. The cell wall permits such transport, being a highly specialized structure that covers the outside of the plant cell. The cell wall performs many functions; it acts as a physical barrier between the cell and the external environment, gives the cell a specific form ensuring mechanical and structural support, balances the internal pressure of the cell, and protects it against pathogenic agents by the release of metabolites. Last but quite not least, it allows the interactions and hydraulic communications among adjacent cells.

The cell wall has a very complex structure and is highly organized; it is composed of several concentric layers that are deposited in a centripetal manner during the growth of the cell.

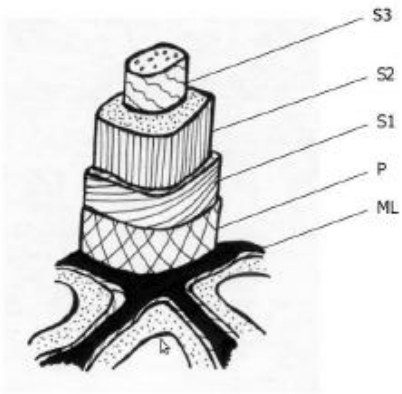

Fig. 13 Structure of a wood cell [12]. S3 secondary wall 3; S2 secondary wall 2; S1 secondary wall 1; P primary wall; ML middle lamella.

In Figure 13 a schematic composition of plant cell wall is reported. The primary wall (P) is constituted by a small part of cellulosic, intertwined fibrils to each other in a disorderly manner. The spaces between the fibrils are filled with amorphous material, hemicellulose, pectin, but especially lignin (65-70%) [89]. The primary wall is quite flexible and relaxes allowing cell growth.

The secondary wall (S) constitutes the majority of the cell wall and is formed mainly by fibrils of cellulose (75% of the total composition); it is deposited in the interstices of the lignin, which confers mechanical strength to the wall. The secondary wall is composed of three layers characterized by a different orientation of the cellulose fibrils and, in some cases, even from a different chemical composition.

Among the primary walls of adjacent cells is present the middle lamella (ML), a thin layer of amorphous material (lignin, pectin and structural proteins) that unites the cells and confers rigidity.

1.7.1 Lignin

Lignin is a complex polymer, whose composition depends on the plant material from which it comes [89]; therefore 'lignins' should be preferred when a general view of the topic is depicted. Structurally, lignin is formed by a complex of aromatic polymers linked together by carbon-oxygen-carbon and carbon-carbon bonds. These are the most resistant to chemical attack. Lignin is a hydrophobic substance and binds chemically and physically the polysaccharide components of the wall, with increased impermeability, mechanical strength and rigidity of the cell wall [90].

Lignin derives from three arylaliphatic alcohols: *p*-coumaryl alcohol, coniferyl alcohol, and sinapyl alcohol, which could be considered the monomers of the polymeric structure of lignin and which differ in the presence or absence of methoxyl groups $–OCH_3$.

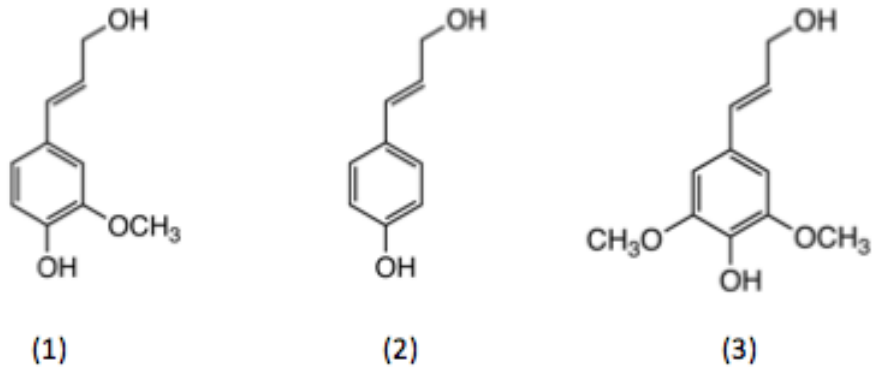

Fig. 14 Monomers of Lignin.: alcohol: *p*-coumaryl (1), alcohol, coniferyl alcohol (2), and sinapyl alcohol (3),

These compounds, collectively called monolignols, share a phenolic hydroxyl, which is responsible for their copolymerization mechanism [91]. These alcohols, synthesized in the cytoplasm, are transported to the cell wall where, in the presence of peroxidase and by the action of the hydrogen peroxide undergo a dehydrogenation with formation of the

corresponding phenoxy radicals. Those at the end polymerize to form at first dimers, and then lignin.

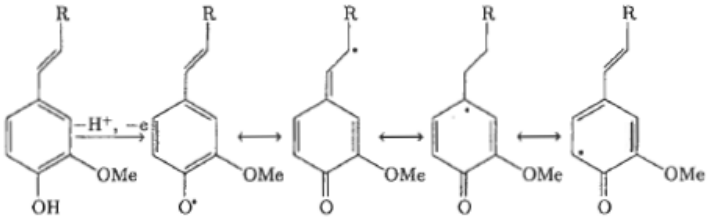

Fig. 15 Phenolic intermediate radicals in the synthesis of lignin

At the same time, formation of cross-links among the growing molecules of lignin it establishes new linkages between the phenoxy radicals and the other macromolecular components of the cell wall [92].

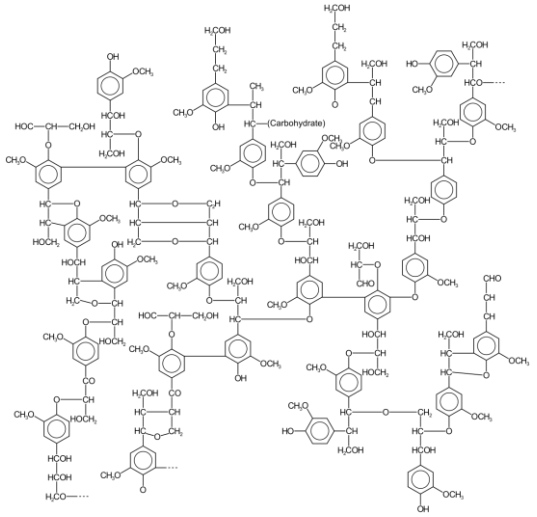

Fig.16 Structure of a hypothetical molecule of lignin.

Looking at this structure, it appears that the lignin, compared to other biopolymers, is hardly biodegradable, for the presence of a 3D very dense texture, given by the different links [92]. These are mainly carbon-carbon bonds or oxygen bridges, which are present in the chains. Lignin is involved, especially, in the substitution reactions, oxidation and hydrolysis. The aromatic nuclei undergo the typical reactions of the benzenoid substrates, that is, the aromatic electrophilic substitution.

Among these processes, the most common are those that take place during bleaching of pulp with chlorine, in the course of paper production, in which the molecular chlorine (electrophilic) rapidly attacks the lignin. The phenolic systems, however, can participate in many reactions, because they are able to give rise to reactive radical, anionic and quinonoid intermediates.

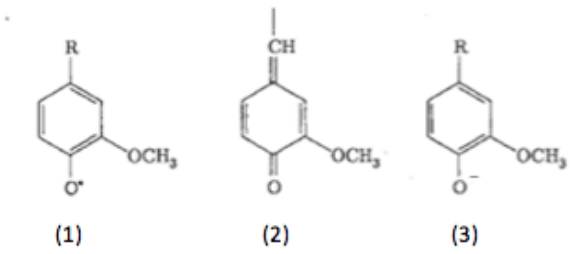

Fig. 17 Reactive intermediates of lignin: radical (1), quinonoid (2) anionic (3).

Due to its macromolecular, heterogeneous, insoluble nature, lignin is not a satisfactory substrate to test LiP and MnP activity, and for the same reasons is unsuitable for testing the bioemulators such as redox active metalloporphines [4]. Veratryl (3,4-dimethoxybenzyl) alcohol is routinely used to test any ‘ligninase’ activity [93] , because it is soluble in water

to an extent enough to avoid the need of any organic cosolvent, is easily available at a low cost, is practically harmless under the experimental conditions used along the catalytic assays. Typically, veratryl alcohol is changed by ligninases into veratraldehyde, which is quantitatively determined through the measure of the absorbance at 310 nm.

1.8 Antifungal drugs

Fungal infections are caused by pathogenic fungi after their penetration and multiplication in host tissues [94].

Antifungal therapy can count on a relatively limited number of drugs, but in recent times, the situation has undergone major changes: up to 1970 based on a few drugs [95], this therapy can now count on different molecules, and this is a considerable progress compared to the past because it offers the physician the possibility of choosing between different treatment options. Fungi are eukaryotic organism, so antibacterial agents are as a rule ineffective [94] .

Systemic antifungal drugs can be classified based on their chemical structure and their action mechanism:

- Azoles

- Macrolides/polyenes

- Echinocandins

The different classes have different spectra of action as well as different pharmacokinetic features and side effects.

1.8.1 Azoles

Azoles (mainly imidazoles) are a large and growing family of antifungal drugs that are able to specifically inhibit a key step in fungal sterol synthesis, that involving the enzyme lanosterol-C-14-alpha demethylase, belonging to the cytochrome P450 family. By this way, ergosterol cannot be produced, and so the resulting damage of the cell membrane leads to the death of the pathogen [96]. Generally speaking, the biodegradation of the antifungal azole within the fungal cell is only poorly known. On the other hand, some of the side effects observed along azole-based antifungal therapy depend on the more or less specific inhibition of hepatic P450 enzymes. Until now, the metabolic fate of these drugs within the human body is largely unknown.

Many azoles are solely useful for topical, dermatological or gynecological applications. Among azoles for systemic use, bifonazole is the main subject of the present study.

2 Experimental

2.1 Materials

All the reagents used were of the best grade available, and were used without further purification. In particular, ARS came from Fluka (cat. No. 05600), Sodium Hydrosulfide Hydrate (Sigma Aldrich cat. No161527), FeTFPP from Aldrich (cat. No. 252913), glutaraldehyde from Fluka (cat. No. 49629, it was as a 50% aqueous solution, mainly containing oligomers in addition to the monomeric aldehyde), MnP from Sigma–Aldrich (cat. No.P–6782), LiP from Sigma–Aldrich (cat. No. 42603), MB from Fluka (cat. No. 66720), PVA from Aldrich (cat. No. 363138, fully hydrolyzed, Av. MW 30,000–50,000), SG 100 from Fluka (cat. No. 60746), Fully hydrolyzed PVA, Av. MW 30,000 – 50,000, was from Aldrich (Milan, Italy, cat. no. 363138) Isopropanol (Sigma-Aldrich 24137), Fumed silica (Sigma-Aldrich 55130) 3 [2 (2-aminoethylamino) ethylamino] propyltrimethoxysilane (Fluka 06666) Diethylene glycol dimethyl ether (Fluka 111-96-6), Sodium cyanoborohydride 1 M solution (Sigma-Aldrich 296943), 4-pyridin carboxyaldehyde (Sigma-Aldrich P62402), Dimethyl sulfoxide DMSO (Prolabo VWR 23486-322), Methylmorpholine (Fluka 109-02-4), Acetic anhydride (Carlo Erba 421491) Hydrogen peroxide (Sigma-Aldrich 7722-84-1), Oxone (potassium hydrogen monopersulfate KHSO5 Sigma-Aldrich 70693-62-8) Methylene blue (Merck 842588) Thionine acetate (Sigma-Aldrich 861340) Azure A (Fluka 11665) Azure B (Fluka 11660) Azure C (Fluka 11667) Silica gel100 (SG) came from Fluka (cat. no. 60746), 5,10,15,20-tetrakis(2,6-dichlorophenyl)porphine-manganese(III) (MnTDCPP) came from Porphyrin System (Lübeck, Germany, cat. no. PO890047), LiP (E.C.1.11.1.14) was from Sigma–Aldrich (cat. no. 42603) Bifonazole (Sigma-Aldrich 60628-96-8), Ammonium acetate

(Sigma-Aldrich 631-61-8), Acetonitrile (Fluka 34967), Ammonium Formate (Fluka 17843), Perfluorobenzophenone (Sigma-Aldrich 853-39-4).

.

2.2 Methods

2.2.1 APS

Aminopropylsilica (APS) was prepared by reacting 10 mmol of (3–aminopropyl)triethoxysilane in 20 mL of dioxane and 10 g of Silica Gel 100 (SG).

The slurry was kept at 80°C overnight. The activated silica was consecutively washed with 0.5 M HCl, with H_2O, with 0.1 M NaOH and again with H_2O. The wet silica was then carefully dried overnight in a vacuum oven at 50°C.

2.2.2 IPS

Firstly, 3–(1–imidazolyl)propylcarbamoyl–3'–aminopropyl–triethoxysilane was synthesized by reacting 2.6 g (10 mmol) of (3–isocyanatopropyl) triethoxysilane and 1.4 g (11 mmol) of *N*–(3–aminopropyl)imidazole in 20 mL dioxane.

The mixture was allowed to react overnight at 25°C, and to this newly synthesized silane 10 g of SG 100 were added. The slurry was kept at 80°C overnight. The activated silica, 3–(1–imidazolyl)propylcarbamoyl–3'–aminopropylsilica (IPS), was consecutively washed with 0.5 M HCl, with H_2O, with 0.1 M NaOH and again with H_2O. The wet silica was then carefully dried overnight in an oven at 80°C.

2.2.3 PSG

PSG was prepared as described above for IPS, except that 4–picolylamine (4–(aminomethyl)pyridine) was used instead of *N*–(3–aminopropyl)imidazole.

2.2.4Silanized Fumed Silica

The fumed silica is silanized: silanes with the general formula $(RO)_3Si–(CH2)_n–X$ were used, where R is typically a methyl or ethyl group, and X represent a functional group. This structure allows grafting different organic functions on the inorganic support.

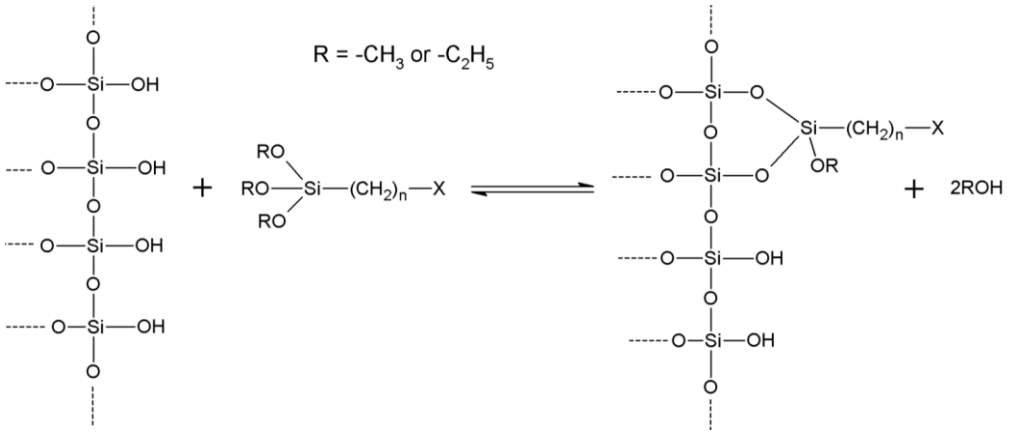

Fig. 18 Reaction between silica and silane

The following silane was used: 3 [2 (2-aminoethylamino) ethylamino] propyl trimethoxysilane. (Fig.19)

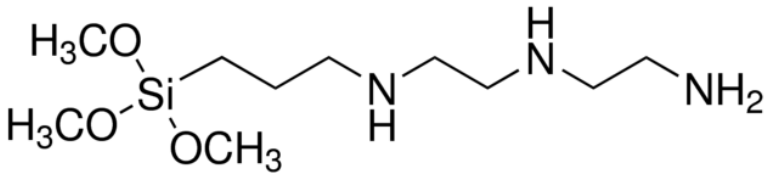

10 g of fumed silica were put in a beaker and suspended in water to form a slurry (fumed silica is extremely fine and many rinsing/decanting cycles with H_2O are needed prior to the subsequent step). Then the slurry was filtered, the obtained wet paste repeatedly washed with isopropanol and finally dried in an oven at 80°C.

The dried fumed silica was treated in a glass flask with a 20% solution of 2[2(3Trimethoxysilylpropylamino)ethylamino]ethylamine, (3[2(2Aminoethylamino)ethylamino]propyltrimethoxysilane) in diethylene glycol dimethyl ether. The slurry was placed in an oven at 80°C overnight.

The silanized silica was washed with 0.1 M HCl, water, 0.1 M NaOH, and finally again with water to neutrality. The wet product coming from suction filtration was then washed with isopropanol and dried in an oven at 80°C.

The product was treated with excess 10% pyridine-4-carboxaldehyde in diethylene glycol dimethylether. The suspension was gently stirred for 20' and then treated dropwise with excess cyanoborohydride in aqueous NaOH, and stirred further for 12 hours. The product was washed with isopropanol and water. The wet paste was filtered by suction and washed again with isopropanol, and finally dried in an oven.

2.2.5 Preparation of the silica-based heterogenized catalysts

The chosen metalloporphine (12mg of FeTFPP or FeTDCP) was dissolved in 1,5 ml of DMSO and the dark brown solution was mixed with 600 mg of the silanized silica. The obtained slurry was slowly inverted end-over-end overnight. Then it was washed exhaustively with isopropanol until no more metalloporphine was extracted; the dark colored product was vacuum filtered and dry at 80°C in an oven. The catalysts were stored

in the dark, at room temperature, until used.

2.2.6 Acetylation of heterogenized silica-based catalysts

For certain experiments, the –NH– groups of the organic arm of the silanized supports had to be acetylated. To this purpose, approximately 200 mg of each carrier containing metalloporphine were treated with 4 mL of diethylene glycol dimethyl ether, 400 μL of methylmorpholine, 800 μL acetic anhydride. The suspension was maintained at 80°C overnight in an oven, and then washed with isopropanol, with water until neutral, and then dried again in an oven at 80°C.

2.2.7 PVA-base heterogenized catalysts

The preparation Fe-TFPP/PP-PVA adduct was performed as already described [97] .

Briefly, aminopropyl cross-linked PVA (AP-PVA) was prepared by treating 500mL of a 10% w/v PVA aqueous solution with 5 mL 4-amino-butyraldehyde diethyl acetal. pH was adjusted to ~3 with 6M HCl, and

then 10mL of glutaraldehyde aqueous solution was added under stirring and the pH adjusted to ~1 with 6M HCl. The obtained gel was kept at 90°C for 1h and finally overnight at 25°C.

The product was ground for 10min at 16,000 rpm with Ultra Turrax , exhaustively washed with water, 0.1M NaOH, water again, 2-propanol, and finally carefully dried at 50°C in an oven.

One gram of the AP-PVA powder was suspended in water and treated with 0.1mL of 4-pyridinecarboxaldehyde.

The pH of the slurry was adjusted to 5 with 0.1M acetic acid/sodium acetate buffer, and 0.5 g sodium cyanoborohydride was added. After 24 h under gentle stirring, the support

was exhaustively washed with 0.1M aqueous glycerol, water, 0.1M NaOH, water again, and 2-propanol. The wet PP-PVA was then carefully dried overnight in a vacuum oven at 50∘ C. The same protocol indicated for metalloporphine heterogenization on modified silicas was applied to fix the chose metalloporphines to the pyridine-functionalized PVA, the sole diference being the cooler temperature (50°C) adopted for drying operations.

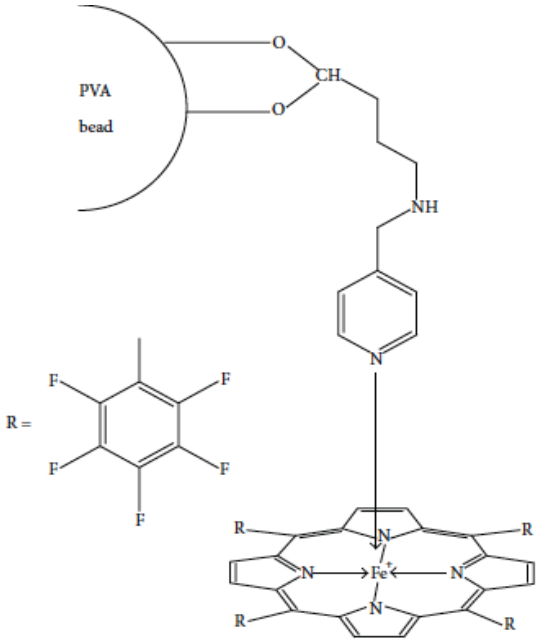

Fig. 20 Structure of the adduct

2.3 Catalytic Assays

2.3.1 H_2S Catalytic Assay.

A mixture containing 10 mg of catalyst , in this case PP-PVA/FeTFPP suspended in 1 mL of 25mM buffer solution containing 10mM NaHS and 45mM aqueous H_2O_2 was kept stirring at 25∘ C in the dark. Blank experiments were performed without one substrate or without catalyst. In a series of experiments, the concentrations of the substrates were varied within a proper range.

After prefixed periods of time, aliquots of the reaction solution (500 μL) were treated with 100 E.U. of purified catalase at 25∘C and used for sulfide and sulfate quantification. In order to test catalytic performance at various pH values, some buffers were used: pH 3, pH 4, pH 5, pH 6, pH 7, and pH 8.

2.3.2 Sulfide and Sulfate Determination.

Sulfide concentration was determined through photometric automatized cuvette test LCK653, using a portable spectrophotometer (Hach-Lange, Germany).

Sulfate was estimated after acidification of the samples (200 μL) with 50 μL 1M HCl. To remove some colloidal sulfur, when necessary, the acidified samples were centrifuged at 12,000 rpm for 15 min. Sulfate analysis was performed through photometric automatized cuvette test LCK153, based on a nephelometric measure.

The catalytic assay for the determination of sulfide has been repeated 8 times to assess the possible multicyclic use of the catalyst.

For certain experiments, horseradish peroxidase (HRP) was used instead of PP-PVA/FeTFPP catalyst (1.5 E.U. total enzyme). The other conditions were kept unchanged.

2.4 Comparison between imidazole- and pyridine-functionalized silicas

The adducts used in these assays are IPS/MnTDCPP and PSG/MnTDCPP.

Routine measurements of catalytic activity were performed through photometric assays. A mixture containing 10 mg of catalyst suspended in 2 mL of 200 mM buffer solution containing 2 mM VA and 8.8 mM hydrogen peroxide, was kept stirring at 25°C in the dark. Increase in absorbance at 310 nm was measured after 30_incubation, to detect the formed

veratraldehyde (ε_{310} = 9300 $M^{-1}cm^{-1}$). ARS bleaching was quantified at 25◦C by spectrophotometric assay: 10 mg of catalyst were added, in a final volume of 2 mL, to200 mM buffer, 8.8 mM H_2O_2 and 0.5 mM ARS. The mixtures were kept stirring in the dark at 25◦C for 30', then pH was adjusted to 7 with 0.2 mL of McIlvaine buffer 1 M (pH 7) and the absorbance decrease at 520 nm was recorded (ε_{520} = 7200 M−1cm−1). Alternatively, the dye azure B was used as the substrate. To a mixture containing 200 mM buffer, 0.88 mM hydrogen peroxide, and 0.01 mM azure B, in a final volume of 2 mL, 10 mg of catalyst were added. After 30' of stirring in the dark, decrease in absorbance at 651 nm was detected (ε_{651}= 48,800 M−1cm−1). For certain experiments, the well-known hydroxyl radical scavenger 0.1 M mannitol was also added. The actual hydrogen peroxide concentration was determined by $KMnO_4$ titration. In a series of experiments, hydrogen peroxide was replaced by Luperox (t-butyl hydroperoxide) as the oxidant, using the same final concentration. The ability of the heterogeneous catalysts to bleach some textile dyes was studied using 10 mg of catalyst in 2 mL of 200 mM buffer solution containing 8.8 mM hydrogen peroxide and a proper con-centration of the selected dye. The routine analyses were performed using the following concentrations of dyes: 0.5 mM ARS, 0.31 mMPNS, 2 mM XO, 0.15 mM MB, 1.5 mM MG, and 1.25 mM MO, according to previously reported protocols [19]. Reaction was monitored photometrically using the λ max and molar extinction coefficients reported in [19]. In order to test catalytic performance at various pH values, some McIlvaine buffers were used: pH 3, pH 4, pH 5, pH 6, pH 7, and pH 8. All experiments were performed both in the absence and in the presence of 50 mM malonic acid and 1 mM MnSO4to assay MnP-like activity. Multi-cyclic runs were performed by regenerating catalysts between consecutive cycles with repeated washings with water and 2-propanol, until no residue of products/substrates was photometrically detected.

2.5 Biomimetic oxidation of thiazine dyes

The five thiazine dyes, namely Thionine, Azure C, Azure A, Azure B, and Methylene Blue, belonging to the homologous series of N-methylated thionine derivatives, were studied as substrates for four heterogenized catalysts prepared as described above. Two alternative oxidizing agents were tested, i.e. hydrogen peroxide and oxone. The oxidation was measured by UV/Vis spectroscopy, assessing the percentage of decolorization, at the wavelength of maximum absorption (in the visible) for each dye.

In order to better evaluate the catalytic activity, in the presence of the two oxidants hydrogen peroxide and oxone, some blanks were prepared excluding the oxidant or the catalyst.

The samples were analyzed at prefixed times. Furthermore, all the tests were carried out at different pH values using the following buffers: sodium citrate buffer 1 M, pH 3; sodium acetate buffer 1 M, pH 5; K_1 / K_2 phosphate buffer 1 M pH 7.

Decolorization was quantified at 25°C by spectrophotometric assay: 5 mg of catalyst were added, in a final volume of 1 mL, 25mM buffer, 8.8 mM H_2O_2 or Oxone and 15 mM the chosen dye.

2.5.1 Control experiments: oxidation of the thiazine dyes in the presence of laccase, HRP, LiP, and MnP

When these enzymes were used, the composition of assay mixtures were changed where appropriate - with the systematic omission of the biomimetic catalyst - as follows: laccase,

23 E.U., 50 mM potassium phosphate buffer, pH 6, no H_2O_2; HRP, 3 E.U., 50 mM potassium phosphate buffer, pH 7, 8.8 mM H_2O_2; LiP, 0.05 E.U., 50 mM sodium citrate buffer, pH 3, 0.176 mM H_2O_2; MnP, 0.02 E.U., 50 mM sodium citrate buffer, pH 3, 0.176 mM H_2O_2, 2mM Mn(II) acetate, dissolved in 50 mM sodium malonate buffer, pH 4.5, respectively.

Moreover, additional experiments where Mn(III) acetate dissolved in 50 mM sodium malonate buffer, pH 6.5, was used as the oxidant, in the absence of other oxidants and biomimetic catalysts, were performed.

2.6 Catalytic Assays for the studied antifungals

The degradation experiments were performed using a mixture containing 0.1 mmol of Clotrimazole or Bifonazole, 1.33 x 10^{-3} mmol of Mn(TDCPP)Cl as the catalyst, 0.2 mmol of ammonium acetate as a co-catalyst, in CH_3CN:H_2O (20 : 1) in a total volume of 2.0 mL, under normal atmosphere at 30°C, in the dark. The oxidant utilized was aqueous hydrogen peroxide 30% (w/w) diluted (1 : 5) in CH_3CN, and 0.05 mmol were added to the reaction every 15 min.

2.6.1 LC/MS analyses

2.6.1.1 Equipment

Chromatographic separation was performed on a High Performance Liquid Chromatography system Thermo Scientific Dionex UltiMate 3000 Rapid Separation LC (RSLC). A Kinetex C8 Column (150 x 2.1 mm, 2.6 µm particle size) was used for the separation.

Chromatographic conditions for Bifonazole: The used isocratic method was perform using a reversed-phase technique, UV monitoring at 210 nm. A mixture of CH_3CN: Ammonium Formate (0.005mol/L) (60:40, v/v) was used as the mobile phase at a flow rate of 0.15 ml per min. The temperature was set to 35'C, and the injection volume was 5ul.

A chromatographic system UltiMate 3000 RSLC from Dionex (Sunnyvale, CA, USA) was used. 5ul samples were injected into a Kinetex C8 Column (150 x 2.1 mm, 2.6 µm particle size), maintained at 35'C. The detection wavelength was set at 210 nm and had given acceptable retention time and good resolution in between Bifonazole and Clotrimazole

2.6.2 % of conversion Bifonazole

To quantify the disappearance of Bifonazole an internal standard
(0.2 mmol perfluorobenzophenone) was used. The conditions of the reaction were equal to those employed in the previous reactions. was perform using a reversed- phase technique, UV monitoring at 210 nm. A mixture of CH_3CN: Ammonium Formate (0.005mol/L) (65:35, v/v) was used such as mobile phase at a flow rate of 1 ml per min., and the injection volume was 20ul.

3 Results and discussions

3.1 Sulfide/H_2S oxidation

PP-PVA/ FeTFPP was able to attain more than 70% conversion of the sulfide in one day (24h). At the same time, noticeable amounts of sulfate were produced in the presence of hydrogen peroxide and catalyst (more than 60% in 24 h). Several combinations of different concentrations of peroxide, sulfide, catalyst, and buffers were tested to optimize the

oxidation of sulfide to sulfate, with the aim of minimizing the production of elemental colloidal sulfur, whose removal is a quite annoying task.

An outstanding feature of hydrogen sulfide is its strong tendency to be changed into elemental sulfur upon mild oxidation. The same is true also for its anions HS^- and S^{2-}, which are more and more present as pH rises, depending on the pKa values of H_2S, ~7 and ~13 respectively. NaHS proved to be an acceptable mother substance to obtain reliable values for the total sulfide in solution under the operative experimental conditions described, and therefore it was used as a source of sulfide along all the present study. A colloidal turbidity arises in aqueous solutions, hindering a reliable analysis of residual sulfide unless such sulfur is not properly removed. The stubborn sulfur colloid is an inconvenience along any operation involving oxidation of hydrogen sulfide and its anions. Elemental sulfur was not apparent during PP-PVA/FeTFPP catalysis at neutral or alkaline pH values, where it was kept into the solution by residual sulfide, as polysulfides S_x^{2-}. These are easily destroyed upon acidification, and the resulting sulfur was removed by centrifugation when appropriate, as noted above. By contrast, the sulfate recovery would not be a problem, even at plant scale, as it might be precipitated as calcium sulfate, dried, and placed in landfills or eventually used as an improver in agriculture.

The reaction was studied within an interval of several hours to take into account the slow, spontaneous autoxidation of sulfide, in particular at alkaline pH values; comparison to suitable blank samples was necessary.

The influence of pH on the efficiency of sulfide removal was studied in the pH range 3-8. Figure 21 clearly shows that the pH optimum for the removal of sulfide is 5, even if a sensible efficiency was still observed at pH 8.

Taking into the due account one of the main aims of this study, namely, the complete oxidation of sulfide to sulfate, the correct stoichiometric ratio (1 : 4 at least) among sulfide

and hydrogen peroxide must be maintained.

The reaction is as follows:

$$H_2S + 4H_2O_2 \rightarrow SO_4^{2-} + 4H_2O + 2H^+$$

Otherwise, oxidation would be incomplete, and formation of colloidal sulfur and/or polysulfides becomes unavoidable. Also, under such conditions, the analytical determination of reactants was uncertain.

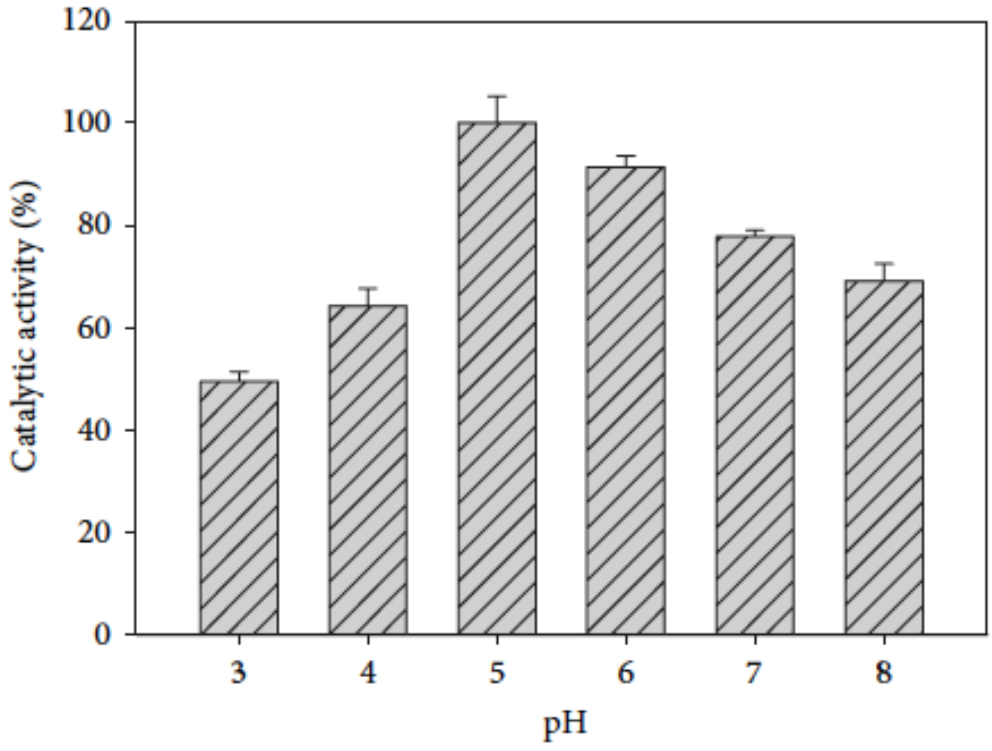

Figure 21 PP-PVA/FeTFPP oxidizes hydrogen sulfide with a pH dependent behavior. 10mg of catalyst reacted in the presence of 25mM buffer solution, 10mM NaHS, and 45mM H_2O_2 (1mL final volume) at 25◦C for 24 h. Results are expressed as sulfide conversion (i.e., sulfide removal regardless of the chemical nature of the oxidation product(s)) (n = 5).

Such a problem of incomplete oxidation simply does not exist in the case of thiols (mercaptans) that are readily and cleanly oxidized to the corresponding sulfonic acids [98] . The organic sulfides (thioethers) are changed into the corresponding sulfones upon oxidation [99] , also under metalloporphine catalysis [100-103].

Thus, clean oxidation of hydrogen sulfide in water to sulfate under mild operative conditions is a serious defiance. Anyway, the feature of concentrate hydrogen peroxide to oxidize hydrogen sulfide at slightly alkaline pH is well known.

Anyway, we have braved the problem with the purpose of a bioinspired catalyst,

namely, an electron-deficient ferriporphin immobilized on to a proper hydrophilic, insoluble support (Figure ??). This was found to be capable of promoting sulfide oxidation to sulfate under small amount of hydrogen peroxide. As we noted , many data exist relative to metalloporphin catalyzed oxidation of sulfide to the corresponding sulfoxides and/or sulfones under proper experimental conditions.

Surprisingly, no data have been found in the literature about hydrogen sulfide oxidation by metalloporphine-based catalysts, under experimental conditions similar to those effective in the case of organic sulfides. The already noted high tendency of H_2S to be oxidized with production of colloidal elemental sulfur, in particular under alkaline conditions, is most probably the explanation of the substantial lack of published studies. Several experiments were in fact necessary to find the optimal conditions to convert hydrogen sulfide to sulfate, taking into the due account that an excessive peroxide concentration could oxidatively destroy the same catalyst. A slight H_2S oxidation was seen also in the blank experiments where the immobilized metalloporphin was present and hydrogen peroxide was omitted from the reaction mixture. This could be explained by means of a hypothetical redox reaction where the ferric porphin was slowly reduced by H_2S to its ferrous counterpart.

Cicle	% Residual activity
1	100
2	91
3	90
4	80
5	78
6	76
7	71
8	63

Table 1 : Sulfate yields obtained under PP-PVA-FeTFPP catalysis. Appropriate blank experiments were carried out in absence of hydrogen peroxide (Blank bar in the figure). 10mg of catalyst reacted in the presence of 25mMbuffer solution pH5, 10mMNaHS, and the indicated H_2O_2 at 25∘C for 24 h (final volume 1 mL) (n = 5).

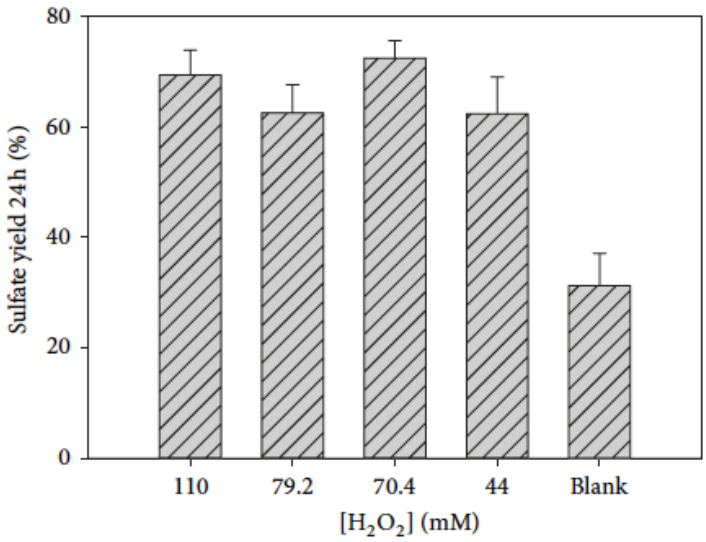

Fig. 23 Multicycle activity of the supported metalloporphine. 10mg of catalyst reacted in the presence of 25mM buffer solution, 10mM NaHS, and 45mMH2O2 (1mL final volume) at 25∘ C for 2h (n = 3).

This could in turn react with molecular oxygen, thus regenerating the catalyst and closing the catalytic cycle. Also, hydrogen peroxide in the absence of the catalyst could oxidize

hydrogen sulfide. However, the yields of sulfate are sharply lower, whereas more colloidal sulfur was formed. All the sulfate yields upon catalytic oxidation compared to the described blank experiments are summarized in Figure 23.

PP-PVA/FeTFPP was also able to save its own catalytic activity after several catalytic cycles. The results summarized in Table 1 show that more than 60% of starting catalytic activity is maintained after 8 cycles.

The biomimetic oxidation of PP-PVA/FeTFPP was still compared with enzymatic catalysis by HRP. The results are summarized in Figure 24. HRP was not able to reach 30% sulfide conversion, even at the highest concentration tested. In the same condition, PP-PVA/FeTFPP allowed a two fold higher conversion, being therefore quite a more promising large-scale alternative for sulfide treatment.

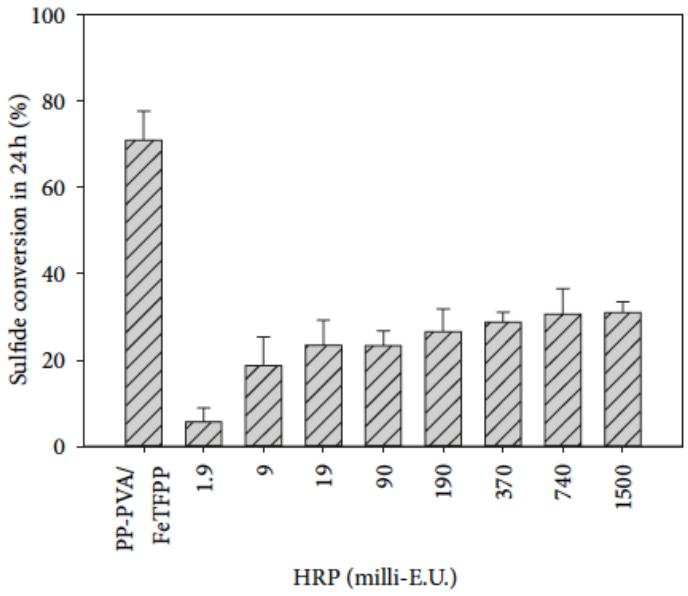

Fig. 24 Comparison between the biomimetic catalysis and horseradish peroxidase (HRP). The indicated E.U. of HRP was incubated in a final volume of 1mL of 25mM buffer pH 5, 10mM NaHS, and 8.8mM H_2O_2. PP-PVA/FeTFPP catalysis occurred in the same conditions described in Figure 3 (n = 5).

With respect to the possible oxidation mechanism(s), some different paths could be hypothesized (Figure 25). A chance is the "classical" peroxidase-like mechanism already proposed for enzymatic sulfoxidation of thioethers [104]. In this path, the *Compound I* analogue Porph+·Fe(IV)=O extracts one electron from H_2S or HS^- leading to radical species $H_2S^{+\cdot}$ or $HS^{\cdot}$, respectively. These could in turn react with the solvent water so triggering further oxidation. Otherwise the radical species resulting from sulfide oxidation reacts with the *Cpd II* analogue PorphFe(IV)=O (oxygen rebound mechanism).The intervention of the solvent should be most probably ruled out by analogy to that found in thioether sulfoxidation by hydrogen peroxide in the presence of the same ferriporphine [105]. Instead, the oxygen rebound mechanism should be the main path leading from sulfide to sulfate, under PP-PVA/FeTFPP catalysis. This hypothesis is strengthened by the observation that thioethers are oxidized to their sulfoxide counterparts by HRP and LiP, with incorporation of ^{18}O in the arising sulfoxides, when the oxygen donor is H_2O_2. Anyway, the arising sulfoxides are formed with low yields, owing to the low tendency of peroxidase to transfer their oxygen from the corresponding *Cpd I* to the substrate [106]. A remarkable exception is that of chloroperoxidases that follow a direct oxygen transfer mechanism [107]. Not surprisingly, the peroxidase we have chosen (HRP) for the reasons of the low costs related to a potential plant scale application was rather unsatisfactory also as a sulfide oxidation catalyst, even when used in high concentrations relative to those of the sulfide substrate.

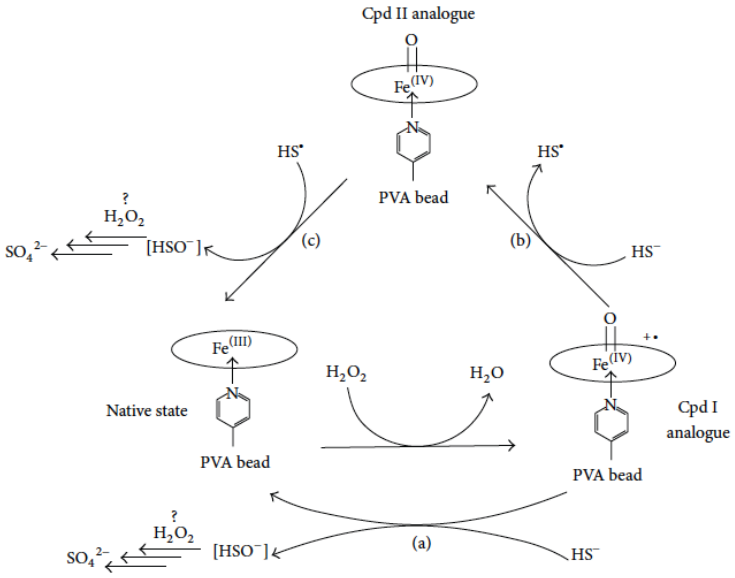

Figure 25: Proposed catalytic path for the immobilized metalloporphin. Path (a) represents the direct oxygen transfer from compound I analogue to sulfide. Paths (b) and (c) represent the rebound mechanism via compound II.

So, the obvious conclusion is that hydrogen sulfide removal by hydrogen peroxide through peroxidase catalysis is not a feasible process. In the case of metalloporphine catalysis a direct transfer of the oxygen atom from the *Cpd I* analogue to the sulfur in sulfide could be envisaged and has been discussed in the literature with concerns to thioethers (path (a) of Figure 25 [106-108]). However, the prevailing view is a rebound mechanism for these substrates [105] (paths (b) and (c) of Figure 25).

In the case of (hydrogen) sulfide, an electron transfer from the (hydrogen) sulfide to the *Cpd I* analogue would be immediately followed by an oxygen transfer from the arising *Cpd II* analogue to the sulfide radical.

Perhaps an extremely reactive and transient sulfenic intermediate HSOH or HSO^- should arise, quickly evolving to more oxidized sulfur compounds and finally to sulfate, most probably by the direct action of excess hydrogen peroxide, possibly without any need of further metalloporphine catalysis.

3.2 Synthesis and characterization of the adducts IPS/MnTDCPP and PSG/MnTDCPP

Imidazole group from histidine side chain is the natural ligand of porphyrins in ligninolytic peroxidases (LiP, MnP, and VP), being therefore the ligand of choice for biomimetic immobilization of synthetic metalloporphines.

However, also pyridine is able to effectively coordinate metalloporphines and positively modulate their catalytic activity [1, 2, 58], mainly because of its higher electron-withdrawing character. As it is common knowledge coordinating imidazole unavoidably succumbs to the oxidizing strength of the catalyst itself, whereas pyridine, though bioinspired and not biomimetic, successfully resists against oxidative degradation. Accordingly, the first aim of the present study has been the preparation of two silica-based supports grafted respectively with imidazole (IPS) and pyridine (PSG). This aim was accomplished by the well-known reaction between primary aliphatic primary amines and alkyl isocyanates. Two organosilanes were synthesized according to the reactions (a) and (b) in Fig. 1, using (3-isocyanatopropyl)-triethoxysilane and N-(3-aminopropyl)-imidazole or 4-(aminomethyl)-pyridine. These N,N-disubstituted urea-organosilanes were then directly used to functionalize plain silica gel, yielding imidazolyl-grafted silica (IPS)and pyridyl-grafted silica (PSG), respectively.

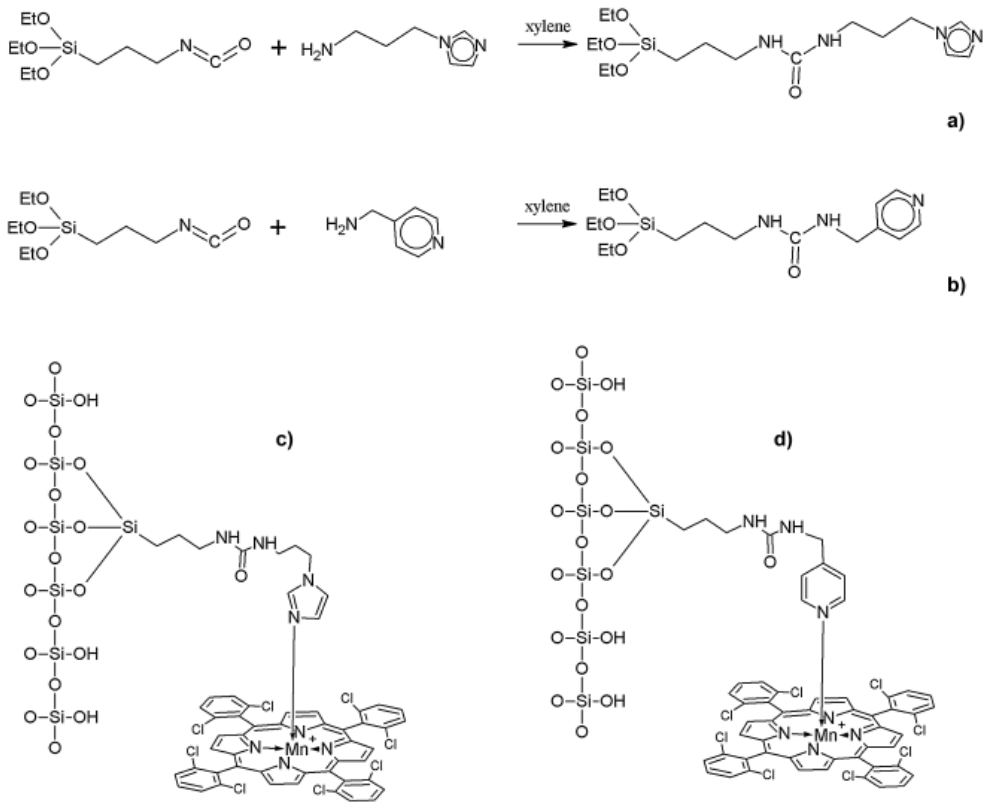

Fig. 26 . Synthesis of (3-[1-imidazolyl]-propylcarbamoyl)-3_-aminopropylsilica (IPS, a) and 4-pyridyl-methyl-carbamoyl-aminopropylsilica (PSG, b). Chemical structures ofthe catalysts described in the present study: IPS/MnTDCPP (c) and PSG/MnTDCPP (d).

Functionalization degree was estimated by total nitrogen determination .

Catalyst	Support functionalization	Metalloporphine loading (umol/g)
IPS/MnTDCPP	207 ± 32	14.6 ± 0.9
PSG/MnTDCPP	52 ± 14	17.9 ± 1.5

Table 2 Functionalization and metalloporphine loading of IPS and PSG. Degree of functionalization is expressed as micromoles of imidazole/pyridine residues per gram of support. The loading of MnTDCPP is also reported as micromoles of metalloporphine per gram functionalized support. n = 3.

The silica support reacted with both silanes, although the loadings observed with imidazolylsilane where sharply higher in comparison to those observed with pyridylsilane. However, PSG loaded slightly more metalloporpine (Table 2). It was impossible to immobilize higher amounts of MnTDCPP, probably due to excessive substituent crowding on the silica surface, affecting both effectiveness of the coordination bond and catalytic efficiency of immobilized metalloporphine. Similar phenomena have been already observed in other immobilization cases [58, 109].

3.3. Catalytic activity of the adducts IPS/MnTDCPP and PSG/MnTDCPP

The main aim of this part of the study was the comparison of imidazole and pyridine as ligands for biomimetic-immobilized metalloporphines. to this purpose, a number of substrates were included, to compare the effect of the two ligands on the catalytic activity. Veratryl alcohol (3,4-dimethoxybenzyl alcohol, VA) is the most common LiP substrate [110] , due to a simple photometric assay involving the formation of veratraldehyde (λmax= 310 nm). Also, its aromatic non-phenolic feature prevents interference by low-redox potential peroxidases. The dye azure B (N,N,N'-trimethylthioninee, AzB) has been suggested as substrate for LiP [111]. In previous reports [5, 112], also Alizarin Red S (1,2-dihydroxy-9,10-anthraquinonesulfonicacid sodium salt, ARS) as a suitable colored substrate for biomimetic metalloporphines. In fact, ARS can be only partially oxidized by one-electron transfer mechanisms.

On the contrary, oxygen transfer route allows its complete oxidation [5]. Thus, ARS permitted to discriminate between these two catalytic pathways. The hydrogen peroxide is the oxidant used by physiological LiP and MnP, but also Luperox (tert-butyl

hydroperoxide) was used for comparison. Luperox is lightly less reactive than hydrogen peroxide, but when the catalysis follows a homolytic mechanism, does not produce the destructive (for the metalloporphine) hydroxyl radical, but instead the less responsive t-butoxy radical [113]. As a primary goal, the effects of pH and Mn^{2+} as a putative redox mediator were studied. The results for VA, ARS and AzB are shown in Fig. 27, using hydrogen peroxide as the oxidant.

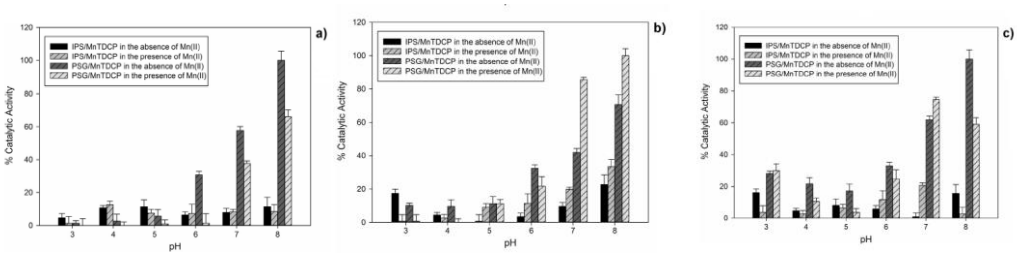

Fig.27.Catalytic activity of IPS/MnTDCP and PSG/MnTDCP is dependent on pH. Data are reported using hydrogen peroxide as the oxidant, both in the absence andin the presence of Mn(II) as redox mediator, with VA(a), ARS(b), and AzB(c) as the reducing substrates. % Catalytic activity is referred to maximum conversion rate obtained for each substrate. n= 3.

Whereas negligible activity was detected below pH 7, a general optimum at pH8 resulted for all tested substrates. Mn^{2+} did not affect catalytic activity, ruling out the possibility of MnP-like activity when the catalysts work on VA and AzB. Only in the case of ARS a slight increase in conversion rate was detected in the presence of this redox mediator at pH 7 (about +50% for PSG/MnTDCP) and 8 (about +25% for PSG/MnTDCP). PSG/MnTDCP was significantly more active than IPS/MnTDCP, as confirmed by the conversion rates in 1 h, at pH 8, reported in Table 3. Pyridine as the ligand led to a 2-fold higher conversion of VA and ARS, and 3-fold higher conversion of AzB.

Substrate	Conversion 1 h (%)			
	IPS/MnTDCPP		PSG/MnTDCPP	
	H_2O_2	Luperox	H_2O_2	Luperox
VA	7 ± 2	4 ± 2	14 ± 3	12 ± 3
ARS	14 ± 3	11 ± 2	35 ± 6	36 ± 4
AzB	16 ± 4	15 ± 3	57 ± 5	25 ± 3

Table 3 Conversion rates in 1 h of IPS/MnTDCP and PSG/MnTDCP using VA, ARS, and AzB as substrates. Catalytic assays were performed at pH 8, both in the presence of hydrogen peroxide and Luperox as the oxidants. % Conversion is the % of initial substrate removed from solution in 1 h. n = 3.

These data were confirmed by kcat values: for instance, IPS/MnTDCP presented a turnover frequency of 0.13 min^{-1}, using VA as the substrate. Under the same conditions, PSG/MnTDCP had a kcat of 0.23 min^{-1}. The products profile greatly differed between the two catalysts. Indeed, PSG/MnTDCP led to about 57% selectivity in veratraldehyde and 11% in veratric acid. For IPS/MnTDCP only 12% of veratraldehyde was detected. In both cases no other products were detectable by using both HPLC/UV and GC/MS, including 2-hydroxymethyl-5-methoxy-1,4-benzoquinone [6]. This is in accordance with the results obtained with similar catalytic adducts [109], where the main part of the products escaped both HPLC and GC analysis, since the oxidation possibly went beyond one-electron oxidation and corresponding veratraldehyde formation, and yielded more polar products such as dicarboxylic acids, oroligomerized/polymerized products.

In Fig. 28 the effects of pH and Mn^{2+} are shown, in the presence of Luperox as the oxidant. Also for these experiments an optimum pH value of 8 was found, and again Mn^{2+} was found to be ineffective as a redox mediator (the only exception was at pH 7 with ARS as a substrate, where an approximately +30% activity was detected for both IPS/MnTDCP and PSG/MnTDCP).

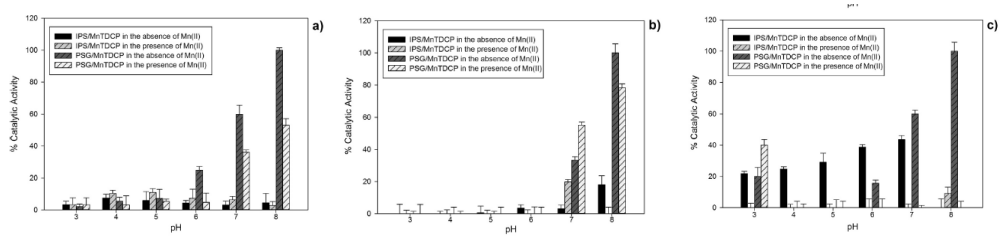

Fig. 28. Catalytic activity of IPS/MnTDCP and PSG/MnTDCP is dependent on pH.Data are reported using luperox as the oxidant, both in the absence and in the pres-ence of Mn(II) as redox mediator, with VA (a), ARS (b), and AzB (c) as reducingsubstrates. % Catalytic activity is referred to maximum conversion rate obtained foreach substrate. n = 3.

The comparison in Table 3, however, shows that Luperox was lightly less reactive in all instances in comparison with hydrogen peroxide. Therefore, hydrogen peroxide should be preferred as the oxidant even for large-scale applications. Indeed, it should also consider that hydrogen peroxide is available at a relatively low price, is completely miscible with water (do not need organic solvents), and releases only the environment of the damage inoffensive products (water and molecular oxygen) during degradation. In both cases, the homolytic cleavage of the *Cpd 0* analog was ruled out, provided that mannitol (a known quencher of hydroxyl radicals) showed no detectable influence towards the catalytic activity (not shown). A large difference between IPS/MnTDCP and PSG/MnTDCP was observed in the oxidation of AzB. Indeed, during catalysis, UV and visible spectral variations regions are completely different (fig.29) .

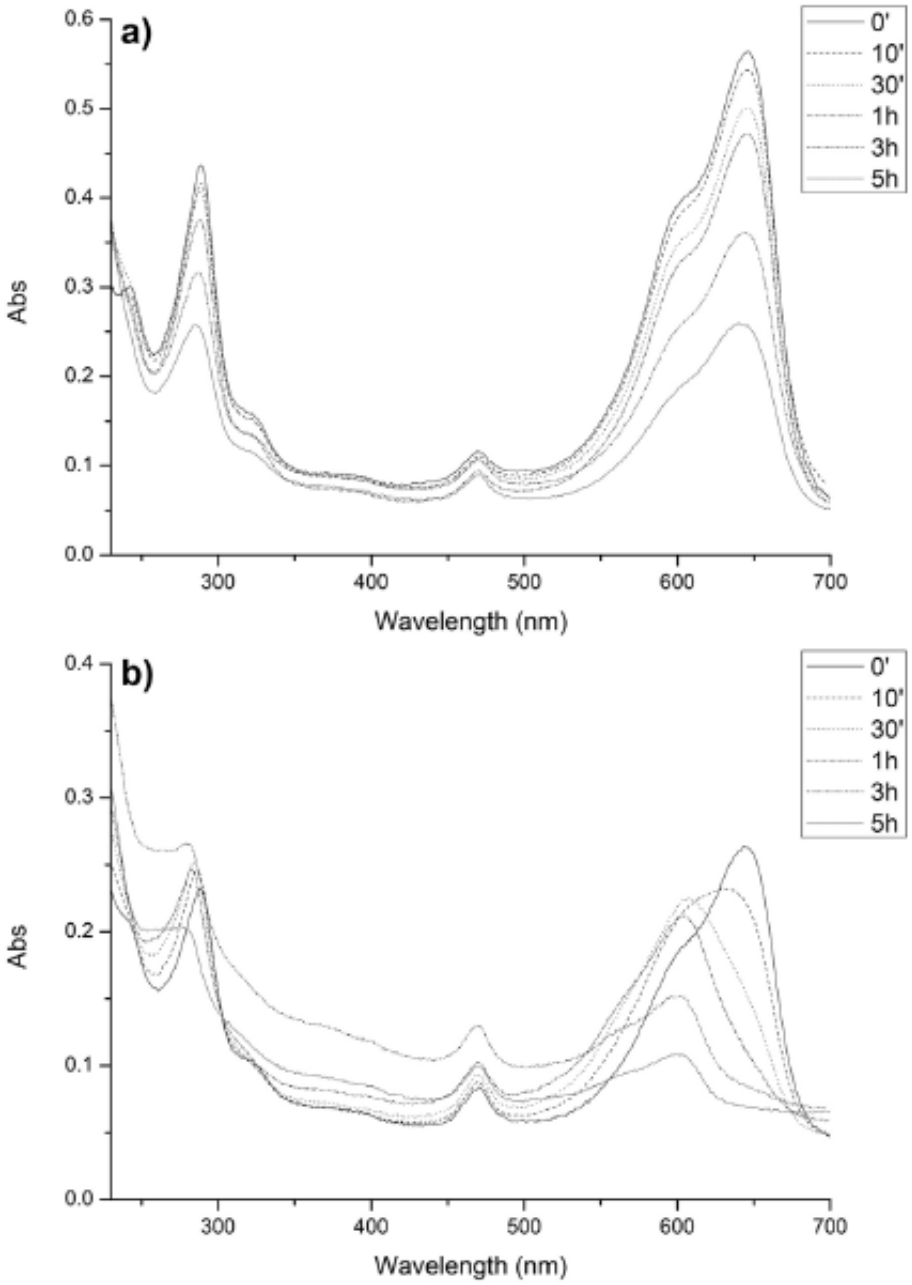

Fig. 29 IPS/MnTDCP (a) and PSG/MnTDCP (b) cause different UV/vis spectral modifications during oxidation of AzB.

This can probably be associated with a different molecular mechanism. Similar differences can be observed during the catalysis of two ligninolytic enzymes such as laccase and LiP, when acting on phenothiazine dyes [110, 113, 114] like AzB. The comparison with spectral change caused by laccase (not shown) suggests a molecular pathway similar to

that found for IPS/MnTDCPP. Whereas LiP has the same spectral pattern of PSG/TDCP.

Immobilized metalloporphines have been investigated for their capacity to oxidize various textile dyes, belonging to different chemical classes (anthraquinones, N-phenyl phenazinium, triaryl methanes, phenothiazines, azo dyes).

The results are shown in Fig. 30

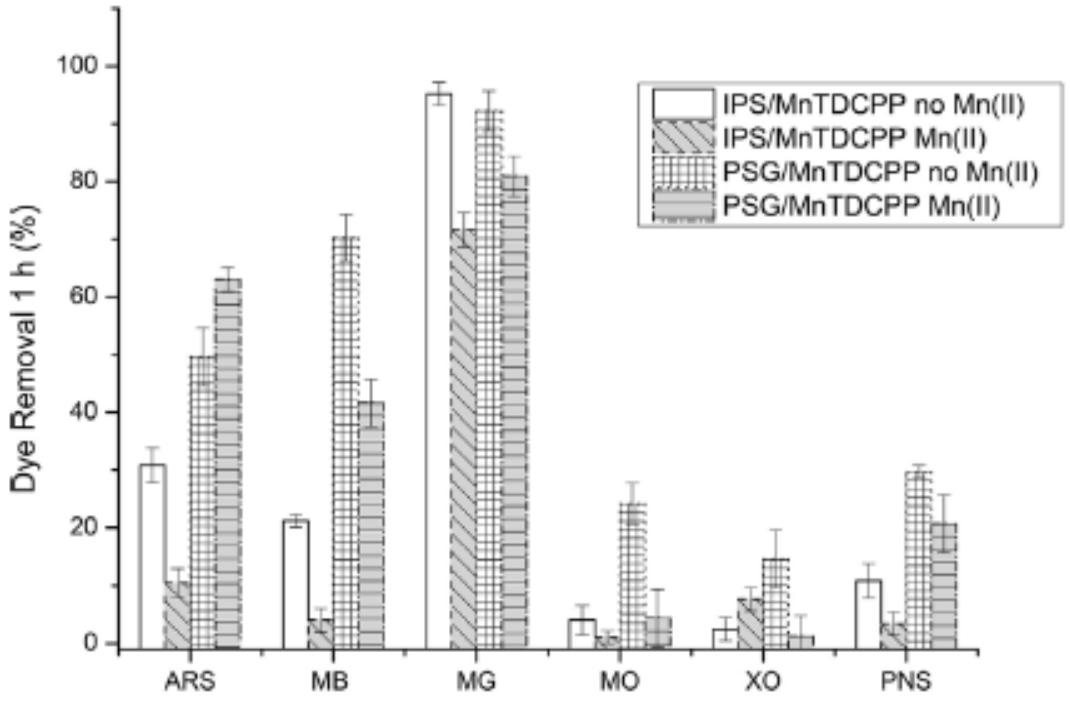

Fig. 30 IPS/MnTDCPP and PSG/MnTDCPP effectively bleach several dyes belonging to different chemical classes. The reactions were performed at pH 8. % Dye removal the % of initial dyes removed in 1 h from solution. n = 3.

All dyes were effectively bleached, suggesting a wide range of substrates for both catalysts. Even in this case, Mn^{2+} did not affect significantly the catalytic activity. Whereas PSG/TDCP confirmed its better catalytic performance. After catalysis, both IPS/TDCPP and PSG / MnTDCPP can be recovered, washed and reused for multiple catalytic cycles. Table 4 summarizes the results obtained for the multi-loop recycling of catalysts using VA,

ARS and AzB. In all cases, after 10 cycles, at least 30% of the starting catalytic activity was maintained. This is a valuable feature for several applications.

Cycle number	% VA conversion		% ARS conversion		% AzB conversion	
	IPS/MnTDCPP	PSG/MnTDCPP	IPS/MnTDCPP	PSG/MnTDCPP	IPS/MnTDCPP	PSG/MnTDCPP
1	100 ± 1	100 ± 1	100 ± 1	100 ± 1	100 ± 1	100 ± 1
2	93 ± 4	66 ± 5	94 ± 3	73 ± 1	100 ± 5	64 ± 5
3	97 ± 2	58 ± 3	89 ± 2	72 ± 4	101 ± 3	57 ± 4
4	93 ± 2	54 ± 1	88 ± 5	73 ± 3	100 ± 2	59 ± 2
5	89 ± 3	52 ± 4	86 ± 3	72 ± 4	89 ± 2	57 ± 2
6	83 ± 4	47 ± 2	88 ± 2	73 ± 3	92 ± 4	58 ± 3
7	60 ± 4	37 ± 4	88 ± 4	72 ± 2	95 ± 3	60 ± 2
8	55 ± 3	30 ± 5	90 ± 4	67 ± 4	72 ± 2	59 ± 2
9	52 ± 1	31 ± 3	87 ± 2	66 ± 3	73 ± 1	38 ± 4
10	50 ± 3	28 ± 2	84 ± 1	65 ± 4	66 ± 2	35 ± 3

Table 4 Multi-cycle recovery of immobilized metalloporhines. For each substrate, the optimum conditions of activity were chosen (compare Fig. 3), using hydrogen peroxide as the oxidant. % Conversion is the % of initial substrate removed from solution. n = 3.

IPS / TDCPP is able, in all instances, to preserve higher catalytic activity for PSG/MnTDCPP, suggesting that imidazole protects more efficiently the metalloporphine from degradation (possibly due in large part to the oxidant itself). The decline in catalytic activity along the various cycles could be in part due to the oxidative degradation of the metalloporphine, and in part to tight adsorption of substrates and/or products on silica supports. Thus, in addition to different surface properties of IPS/MnTDCP and PSG/MnTDCP (possibly leading to differential substrates/products adsorption), these findings could be explained taking into account the higher electron-withdrawing effect of pyridine, if compared to imidazole. This effect may enhance redox potential of the immobilized MnTDCP, making more responsive (to say, more electrophilic) the *Cpd I* analogue. Nevertheless, this increased reactivity could also make the porphine macrocycle more susceptible to nucleophilic attack, leading to quicker catalyst degradation. Therefore, it is not surprising that MnTDCP is more stable against oxidative degradation when ligated

through imidazole. Under all the tested conditions, no measurable elution of MnTDCP and/or of other manganese species was found.

3.4 Molecular mechanism insights

The similarity of the spectral changes observed during the laccase action, on AzB and that of the IPS/MnTDCP on the same substrate speaks in favor of a mechanism of oxidation of an electron promoted by the bio-inspired catalyst, entirely similar to that well known for laccase and "classical" peroxidase such as HRP. In fact, laccase - which belongs to the so-called Blue Multi-Copper Oxidases (BMCO) - usually contain a tetracupric cluster [115] , wherein a type I cupric ion is devoted to abstract one electron from an electron-rich appropriate substrate (usually polyphenols or even aromatic amines, aminophenols, or so on). Overall, the type I copper cycles between the cupric and cuprous states, whereas dioxygen is specifically bound within a tricopper cluster (one type II and two coupled type III ions [29]) and gradually reduced to water [116]. In other words, any interaction of laccase at the same time with reducing agents and dioxygen is avoided, and the formation of the product(s) is essentially driven by the particular nature and reactivity of the radical resulting from the substrate itself. Of course, a direct reaction between the radical and molecular oxygen excess substrate could happen, but the enzyme does not directly influence the case. Completely different is the case of heme peroxidase, which form *Cpd I* as a key intermediate in the oxidation/oxygenation of the substrate: this is a high-valent ferryl Fe (IV)=O derivative of heme, also showing a radical character, hosted by the porphyrin macrocycle [1].

Cpd I is a strong oxidizing agent, and its ability to transfer its oxygen atom to reducing substrates such as sulfides, alkenes, and in general to activated C-H bonds is well known. [117, 118].

In peroxidases, oxygen transfer is a reaction almost negligible in comparison with the 'usual' one electron transfer; but, things look very different in the case of high potential peroxidase (like Lip and MnP), peroxygenases, and P-450 enzymes [119], wherein the transfer of oxygen is important and in some cases the only observed way of action. This transfer in the majority of cases occurs through an 'oxygen rebound' mechanism where the *Cpd I* pulls an electron from the substrate; the arising radical does not abandon the active site of the enzyme, and quickly reacts with the formed *Cpd II* [1, 120]. The oxygen transfer then follows, thus restoring the enzyme resting state and releasing the oxygenated substrate. This mechanism could explain the action of LiP on AzB, as shown in the present study, where the spectral pattern observed during LiP action on AzB is very different from that found in the presence of laccase. Due to the obligate way of action of laccase, based on one-electron abstraction from the substrate, the different pattern observed with LiP can be explained only by a different mechanism, i.e. an oxygenation going through the oxygen rebound mechanism. This seems quite reasonable and most probable. The unique 3D structure of LiP justidfies its higher redox potential in comparison with horseradish peroxidase. For the PSG/MnTDCP, the main features of the pyridyl moiety must be kept into the due account; contrarily to imidazole, pyridine is a typical electron-poor heterocycle, however capable of donating its electron couple on the nitrogen atom to the metal ion at the center of the porphine. In this way, a typical sigma complex is formed. Anyway, pyridine (more easily than imidazole) could accept electron density from the metal ion into its anti-bonding π orbitals. This stabilizes the resting state of the metalloporphine complex, in comparison to the high-valent states *Cpd I* and *II*, that

explains the greater oxidizing power of PSG/MnTDCP in comparison with IPS/MnTDCP (in accordance to recent evidence observed in homogenous phase), and the different mode of action, favoring oxygen transfer in detriment of the simple one-electron transfer. Anyway, a more pronounced oxidizing power is the responsible of the fast self-destruction of the pyridyl-bound metalloporphine during the multi-cycle experiments. The same evaluations could explain the different behavior oft he two catalysts toward VA oxidation. Indeed, the imidazole-based system in this case generates only a small amount of veratraldehyde, together with a mixture of unknown products. One could hypothesize which the arising *Cpd II* is not reactive enough to favor electron abstraction giving veratraldehyde passing through hydration and deprotonation reactions. Instead, oligomers and/or other degradation species derived from the one-electron abstraction from VA could reasonably be the favored products. In the case of the pyridine-based catalyst, the large oxidizing power of both *Cpd I* and *II* presumably lead to a 'regular' oxidation of VA to the corresponding aldehyde, with a reaction pathway paralleling that found in the LiP-catalyzed reaction [121]. Surprisingly, under the chosen experimental conditions, no significant amounts of the well-known byproduct, 2-hydroxymethyl-5-methoxy-1,4-benzoquinone was found, regardless to the peculiar catalyst was used. As a point of fact, neither turbidity nor discoloration of the supernatant was observed (different from imidazole-based catalyst), thus suggesting that a fraction of the arising aldehyde was further oxidized to veratric acid and possibly through a 'direct' oxygen transfer to muconic derivatives and/or very polar degradation products (as observed for other metalloporphines-based systems [122, 123]), escaping both HPLC and GC–MS analyses. Equally undetectable could be polymerization products arising from quinones via radical coupling.

3.5 Oxidation of N-methylated thionines

The aim of this part of the study was to verify the ability of two bioinspired catalysts to oxidize some thiazine dyes, belonging to the thionine family.

The catalysts were immobilized on functionalized fumed silica, where the silane arm was chosen in a manner that ensures the presence of net positive charges along the space arm joining the silica support and the pyridyl end. Such a strategy minimizes any undesired unspecific adsorption of the cationic dyes tested by the potentially polyanionic silica. The combination of the silane coating and the positive charges along the silane space arms generates a Coulomb's repulsion just preventing adsorption phenomena. For certain experiments, the catalyst was acetylated to abolish such positive charges, to evaluate possible changes in catalytic activity and/or in substrate/catalyst interactions.

Experiments were carried out at different pH values and using two oxidizers, i.e. hydrogen peroxide and Oxone. Two different metalloporphines were used: FeTFPP and FeTDCP. The results are encompassed in Figures 32, 33, 34, 35, 36, and are expressed as percentages of decolorization, measured at the λmax values for each dye (Table 5).

Dyes	Wavelength λmax
Thionine (Tio)	598 nm
Azure C (Az C)	620 nm
Azure A (Az A)	626 nm
Azure B (Az B)	648 nm
Methylene Blue (MB)	660 nm

Table 5 Dyes and their rispectives Wavelength λ max

The obtained results show that the four catalysts tested had a particularly complicate behavior that has been explained only to a certain extent, whereas some data are still waiting for a convincing explanation.

First of all, hydrogen peroxide shows its best performances at lower pH, and therefore a very efficient catalysis is shown at pH 3, dramatically dropping down at pH 5. Data collected at pH 7 are not too different from those relative to pH 5. This is not surprising, as it is common knowledge that biomimetic/bioinspired ferriporphines give their best performances at quite low pH, therefore paralleling the Class II peroxidases in such a behavior [124]. Low pH values strongly favor protonation of *Cpd 0* analog, thus causing expulsion of water and formation of *Cpd I* analog. By contrary, higher pH values leave *Cpd 0* analog in its uncharged form, which easily undergoes homolytic fission of the peroxide bond leading to *Cpd II* analog. When working with H_2O_2, the two catalysts based on FeTDCP are invariably the most active, regardless to pH, individual dye, and acetylation or no acetylation of the bridging silane space arm. Other differences among different dyes and different catalysts at pH 5 and pH 7 are poorly significant, whereas relatively sharp differences were observed at pH 3. Non-acetylated FeTFPP-based catalysts became less and less active with increasing of the methylation extent, with the somewhat surprising exception of the fully methylated homolog, MB. In principle, thionine and the Azures A, B, and C may undergo both ET or HAT oxidation pathways, and a decrease in oxidation extent as methylation degree increases seems reasonable if a HAT mechanism prevails. However, an unexpected increase in oxidation efficiency was observed with MB, which cannot undergo any HAT mechanism. The obvious conclusion is that for this dye, under the indicated experimental conditions, an ET mechanism must operate, preceding a putative oxygen rebound step, in turn preluding to dye destruction. Alternatively, one could envisage a relatively efficient direct oxygen transfer from *Cpd I* analog to MB, when

a (less efficient) side reaction going through a HAT mechanism cannot take place. Acetylation of the supports produces a sharp adverse effect towards catalytic efficiency, again with the outstanding exception of MB, whose bleaching is not significantly influenced by acetylation. The reasons of this unexpected behavior of MB are still unexplained.

Oxone is a very strong and reactive oxidizer, whose action mechanism in the presence of catalytic amounts of redox active metalloporphines is well known [124]. It can form a *Cpd 0* analog PorphFe(III)–O–O–SO_3^-, which readily undergoes a heterolytic fission of the peroxide bond forming *Cpd I* and releasing sulfate ion. In other words, homolytic fission and *Cpd II* formation is strongly disfavored. Also in the absence of any catalyst, oxone is a very strong and reactive reagent, capable of rapidly bleaching a wide range of different organic compounds. Therefore, a time-consuming and tedious search of suitable experimental conditions, capable of eliciting the putative catalytic abilities of the studied catalyst was necessary, to build up consistent protocols based on a judicious choice of the blank experiments.

As a general observation, in spite of the fact that Oxone was able to rapidly bleach all the thionines under study, even in the absence of any added catalyst, some important differences were observed. First of all, oxone was constantly much more reactive with FeTFPP-based catalysts as it was with FeTDCP-based catalyst. This effect was lower at pH 3 and higher at pH 7, where the presence of FeTFPP was not influent towards dyes bleaching (Oxone alone bleached all the tested dyes at all the tested pH values). Perhaps, the bulky 2,6-dichlorophenyl substituents in the latter at least in part disfavor the approaching the central iron ion by the monopersulfate ion, whereas this hindering effect does not operate when the oxidant is the small H_2O_2 molecule. The influence of different pH values towards the bleaching reactions is less important with respect to that observed

when operating with H_2O_2, although pH 3 seems again the optimum value. With, oxone at pH 3, acetylation of the supports has constantly a favorable effect on the FeTDCP efficiency, which equaled that of FeTDCP, again with the noticeable exception of MB. The FeTFPP-based catalyst efficiently bleached this dye, whereas the acetylated FeTDCP-based catalyst was quite inefficient. The reasons of this behavior are unknown.

At pH 5, the difference between FeTFPP- and FeTDCP-based catalysts became more evident, again with the exception of MB. With this dye, the catalytic efficiency of the FeTFPP-based catalyst unexpectedly dropped to zero. The reasons of this behavior are again unknown.

At pH 7, non-acetylated FeTDCP-based catalyst was invariably and totally inactive, whereas its acetylated counterpart worked with moderate efficiency. With concern to FeTFPP-based catalysts, the non-acetylated forms showed a moderate activity, which was noticeably raised upon acetylation. As ever, MB behaved quite differently: In that case, acetylated FeTFPP-based catalyst showed only a moderate activity, whereas acetylated FeTDCP-based catalyst was fully active. Again, the reasons of this behavior are unknown. For a tentative explanation, perhaps the already underlined, different acid/base properties of MB in comparison to the other partially N-methylated thionines should be taken in the due consideration: in fact, the positive charge of MB is independent on pH within the studied range, whereas the partially methylated dyes could deprotonate (so loosing their charge) as pH rises. basicity of the compounds presumably increases with increasing the methylation degree, with a sharp jump for MB that cannot be deprotonated even at high pH values.

Thionines were scarcely sensitive to enzymes such as laccase, LiP, and MnP. Bleaching was limited and proceeded very slowly, so the corresponding results have not been reported here.

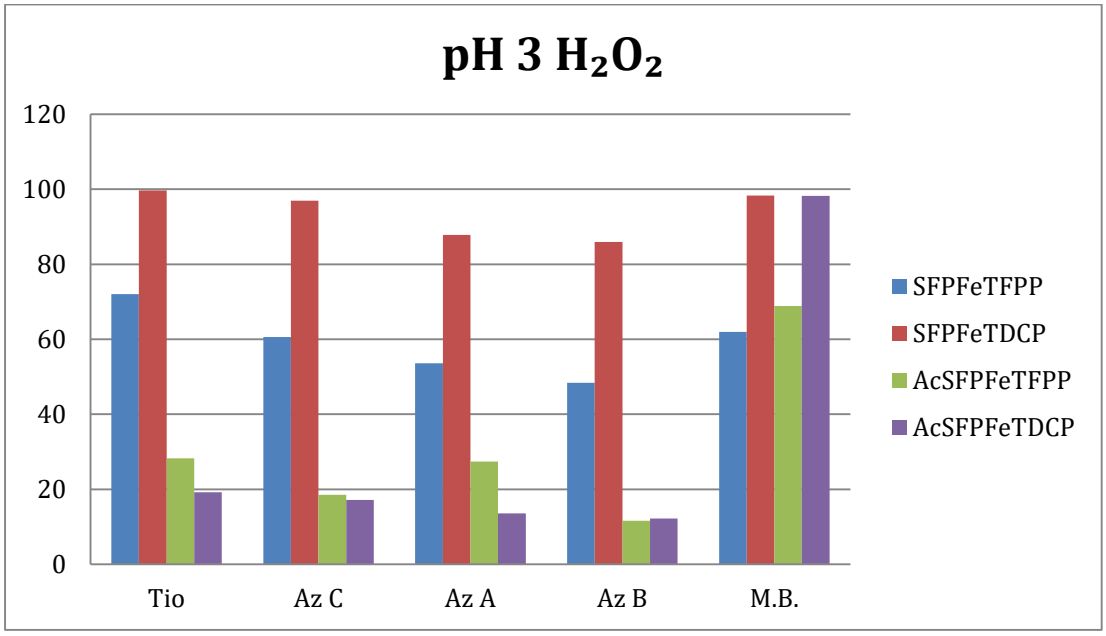

Fig.31

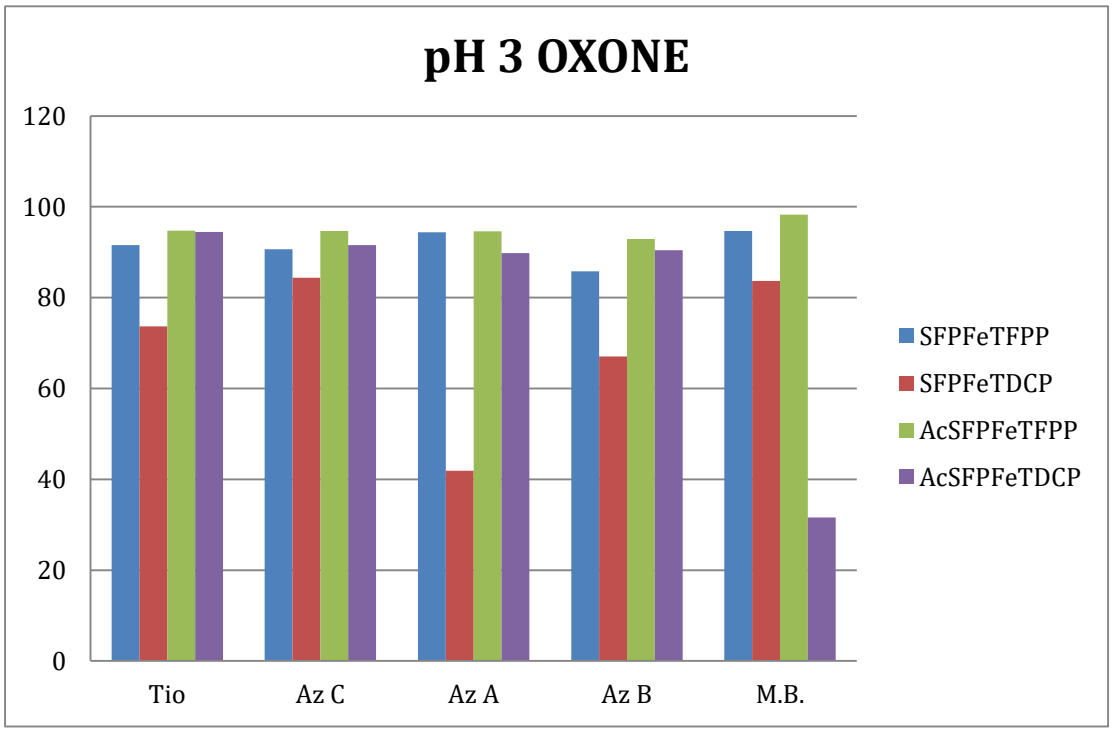

Fig.32

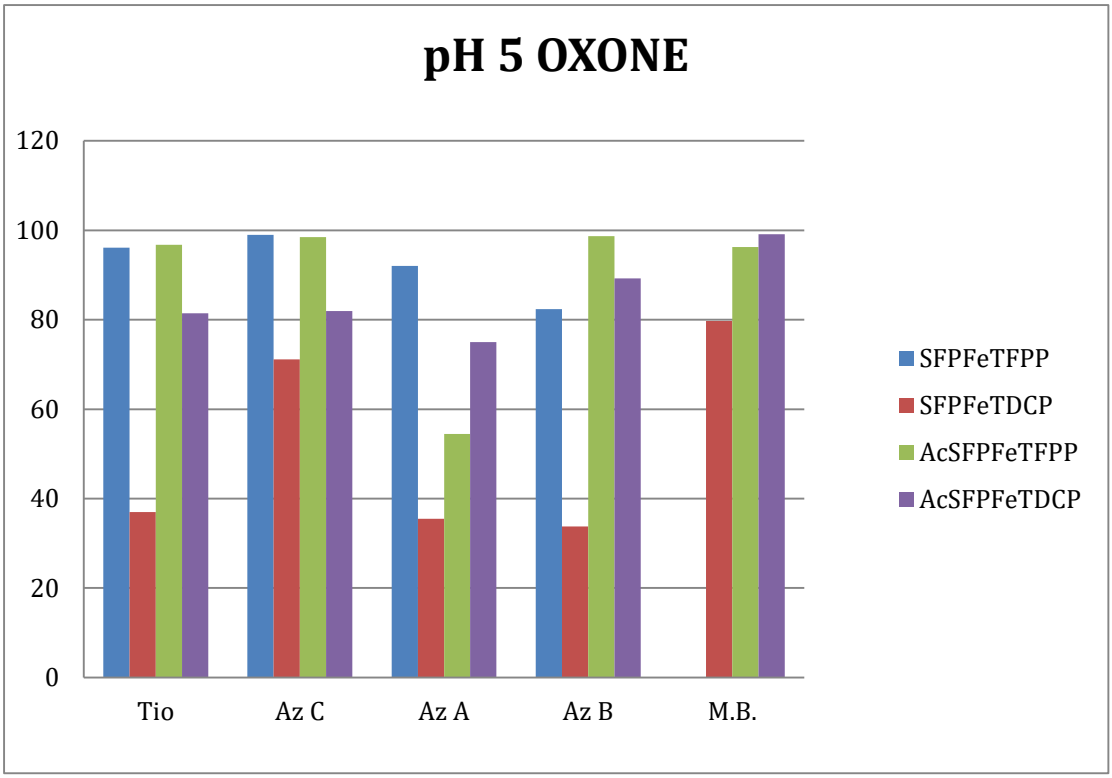
pH 5 OXONE
120
100
80
60
40
20
0
Tio
Az C
Az A
Az B
M.B.
SFPFeTFPP
SFPFeTDCP
AcSFPFeTFPP
AcSFPFeTDCP

Fig. 33

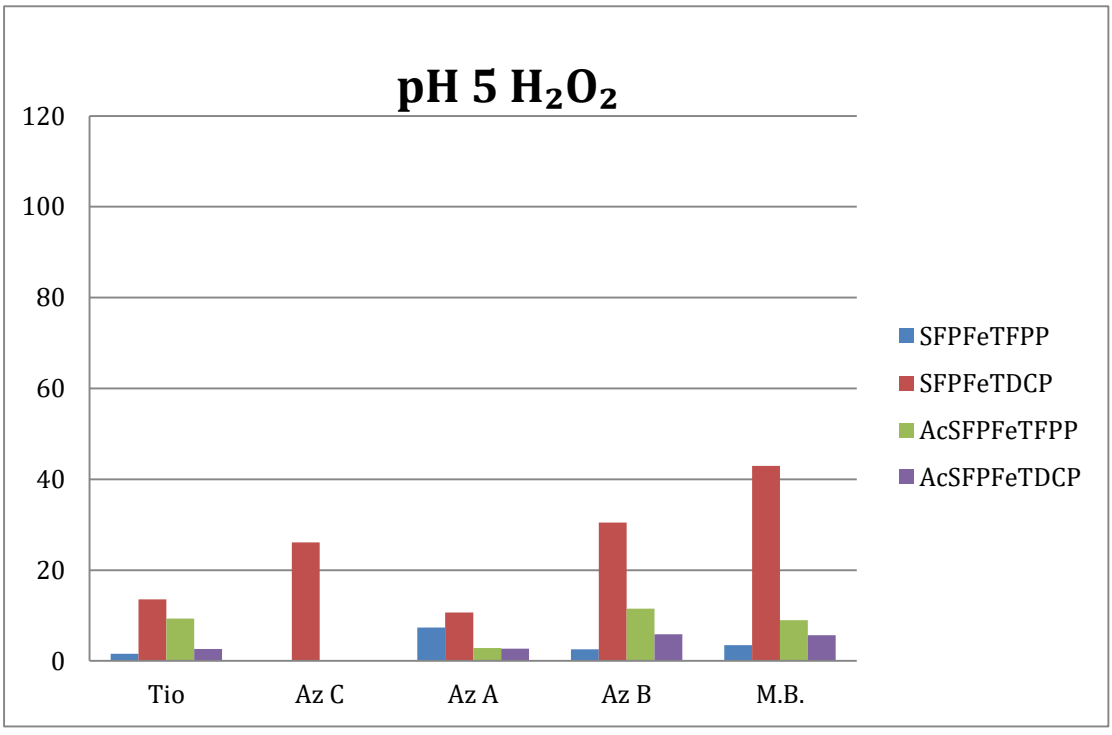
pH 5 H2O2
120
100
80
60
40
20
0
Tio
Az C
Az A
Az B
M.B.
SFPFeTFPP
SFPFeTDCP
AcSFPFeTFPP
AcSFPFeTDCP

Fig. 34

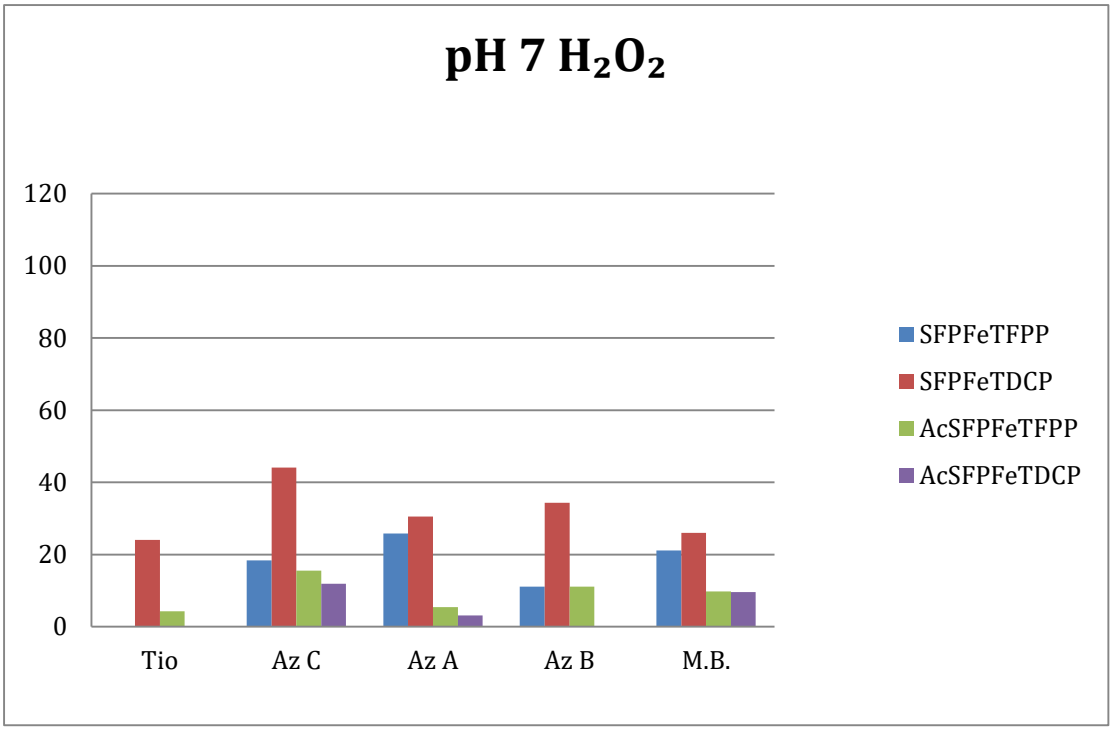
pH 7 H_2O_2
120
100
80
60
40
20
0
Tio
Az C
Az A
Az B
M.B.
SFPFeTFPP
SFPFeTDCP
AcSFPFeTFPP
AcSFPFeTDCP

Fig. 35

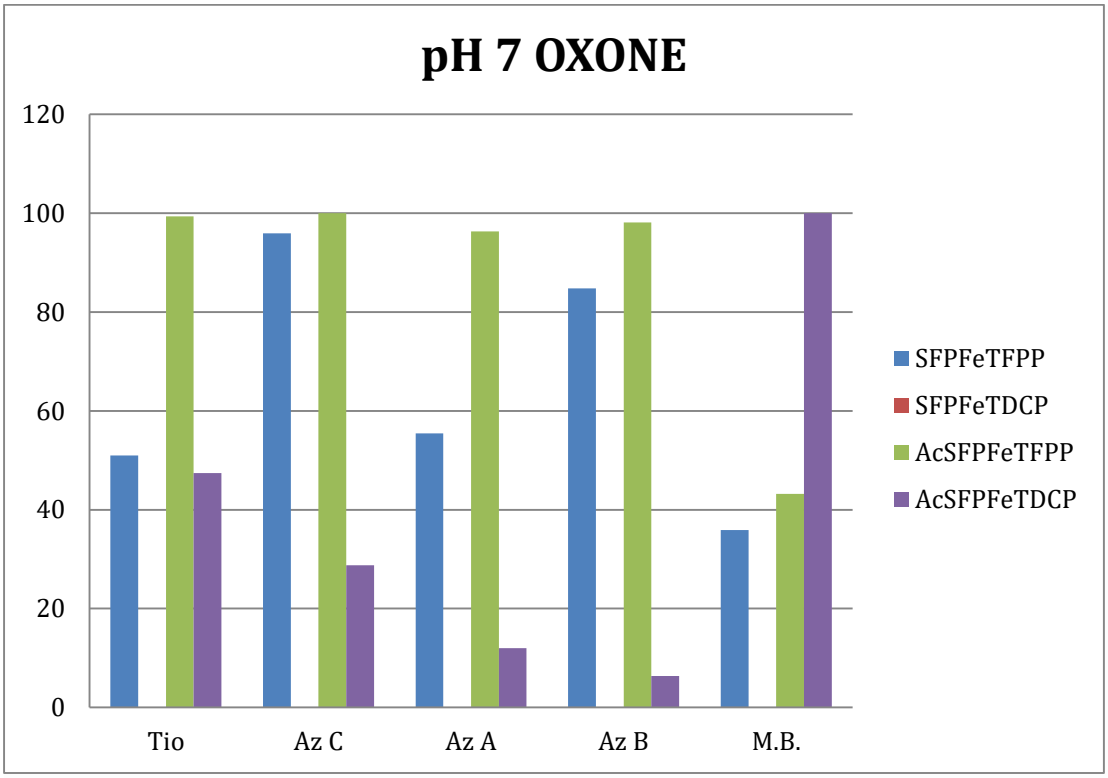
pH 7 OXONE
120
100
80
60
40
20
0
Tio
Az C
Az A
Az B
M.B.
SFPFeTFPP
SFPFeTDCP
AcSFPFeTFPP
AcSFPFeTDCP

Fig. 36

3.6 Antifungal drugs

Metalloporphines are recognized as excellent catalysts for oxidation reactions as biomimetic/bioinspired models of enzymatic activities such as those of cytochromes P450 . Besides, these synthetic models are helpful to understand the behavior of pharmaceuticals in the environment, and to predict drug metabolism by cytochromes P450 [125] .Thus, biomimetic models could allow the production of metabolites or metabolite candidates, and even the isolation and identification of unstable intermediates.

The oxidation reactions of bifonazole (*m/z 311*) using the selected manganese(III) porphines as homogeneous catalysts were performed with progressive additions of diluted H_2O_2, under normal atmosphere, in a mixture of acetonitrile/water at 30°C. The reactions were monitored by reverse-phase HPLC and the conversion of the substrate was determined by LC/MS using

perfluorobenzophenone as internal standard. The degradation of the substrate is 100% after 2h.

The addition of H2O2 was stopped when no further conversion of the bifonazole was observed. During the reaction, four possible products/metabolites were obtained. Two of them could be hydroxylated forms (*m/z* 305; 327) where we are proposed two possibilities for both eventually product and the others seem to have suffered oxidative cleavage (*m/z* 258; 287)

The products were studied by HPLC and characterized by mass spectrometry.

Products	Reaction time (min)	Retention time (min)
258	(60) (90) (120)	(8.0)
287	(60)	(3.02)
305	(60) (90) (120)	(4.88) (4.87) (4.88)
311	(0) (30) (60) (90)	(7.08) (7.11) (7.15) (7.11)
327	(0) (30) (60)	(5.22) (5.22) (5.23)

Table 6

This table shows the fragmentation of the products obtained.

Range of time (min)	m/z	MS 2 major ions	MS 2 minor ions
7.7 - 8	258	241; 181; 180; 155; 104;	257; 241; 230; 223; 216; 201; 185; 180; 168; 155; 148; 132; 107; 104; 86; 77;
3.15 - 3.5	287	243;	272; 255; 241; 228; 217; 199; 191; 168; 160;
4.65 - 5.1	305	287; 263; 246; 245; 113;	276; 269; 261; 254; 231; 185; 137; 123;
6.9 - 7.7	311	293; 243; 157;	283; 275; 269; 265; 252; 233; 225; 202; 191; 183; 175; 161; 142; 130; 113; 97;
5 - 5.5	327	309; 173; 157;	309; 280.6; 271; 195; 183; 173; 156.6;
3.15 - 3.5	375	358; 307; 243;	

Table 7

As shown in the Figure, bifonazole was rapidly transformed, with the concomitant formation of several degradation products. The disappearance of the substrate was fast, and RP-HPLC showed a conversion almost complete after 2 h. Positive Electrospray Ionization Mass Spectrometry (ESI-MS+) analysis was then carried out.

The progress of the reaction has been monitored by means of two techniques: TIC (total ion current) and UV / Vis spectrometry.

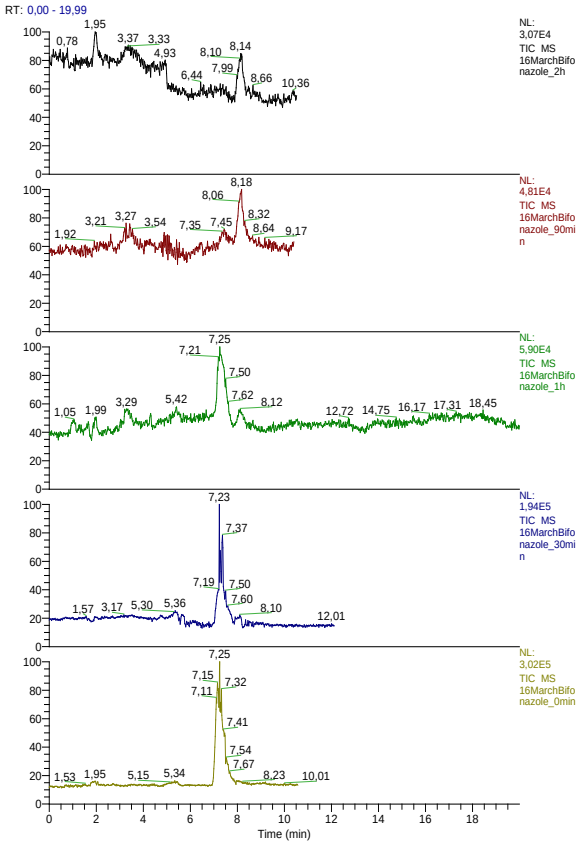

TIC chromatograms

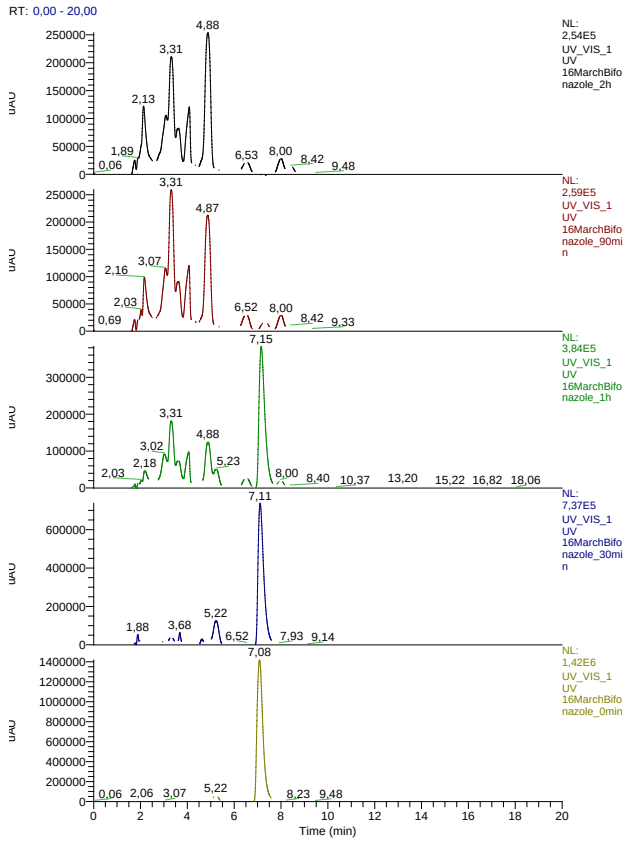

UV/Vis Chromatograms

In the figure 37 the structures of the possible products are shown:

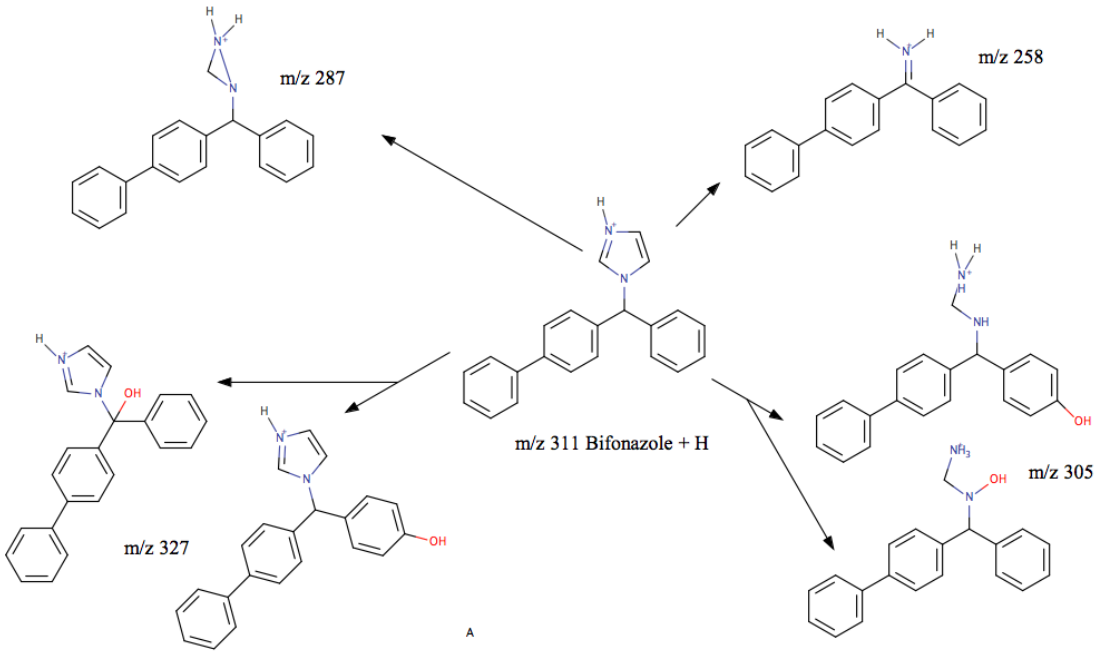

Fig. 37

Planned future work will fully assess and identify the product pattern, and the study will be extended to other azole antifungal drugs drugs.

These preliminary results show that biomimetic/bioinspired metalloporphines, by emulating enzymatic activities of the cytochrome P450 family, could help better understanding the metabolism of azole antifungal drugs both within the fungal cell and in the host organisms.

4 Conclusions

Oxidative approaches towards removal of pollutants are not currently featured by enough efficiency and inexpensiveness. Accordingly, in order to decrease environmental impact and economical costs of industrial processes, new methods need to be proposed.

In this perspective, during this study several catalysts have been developed, using suitable metalloporphines mimicking peroxidase and peroxygenase catalysis.

Emulation of these enzymes was achieved by grafting on inexpensive, hudrophilic supports (such as SG, SF and PVA) coordinating groups like imidazole and pyridine, resembling heme coordination in active site of peroxidases. In particular, hydrophobic FeTFPP gave optimal results when coordinated by pyridyl functions, leading to real LP structural emulation. We have shown the ability of that commercial metalloporphine, when immobilized in this way on to a cross-linked functionalized hydrophilic polymer (PP-PVA) to catalyze hydrogen sulfide oxidation to sulfate, under very mild operative conditions and avoiding the formation of significant amount of elemental sulfur. Therefore, a diluted and nearly neutral hydrogen peroxide solution could be a tool to accomplish the oxidation in the presence of the described heterogenized ferriporphine. Biomimetic adduct also led to better catalytic performances than its enzymatic counterpart. PP-PVA/FeTFPP could be therefore a feasible alternative also in the large-scale process of H_2S removal.

Both imidazole- and pyridine-functionalized silica-based supports have proved able to effectively heterogenize MnTDCPP, mimicking the active site of ligninolytic peroxidases and peroxygenases. Anyway, significant catalytic differences turned out, since pyridyl-immobilized metalloporphine (PSG/MnTDCPP) led to higher conversion rates. Such results give precious insights about the role of the ligand in biomimetic immobilization of metalloporphines. Not surprisingly, the electron deficiency of pyridine resulted in a higher

catalytic activity of PSG/MnTDCPP (owing to the higher oxidizing power of the *Cpd I* analog). Unfortunately, this higher reactivity also turned out in higher instability of PSG/MnTDCPP, suggesting imidazole as the ligand of choice for more stable catalysts. Very different product pattern and mechanisms of catalysis also emerged. The specific electronic features of pyridine were suggested to explain also the proposed different mode of action, possibly favoring oxygen transfer instead of one-electron transfer. These outcomes should allow to more rationally design the supports for immobilization of metalloporphines, depending on the specific requirements of the reactions to be catalyzed. As regards the porphines immobilized on to fumed silica as the support, FeTFPP FeTDCP have been described.

The obtained results show a good catalytic activity of the catalysts at pH 3, while the increase of pH leads to a decrease of efficiency in the bleaching of industrial thiazine dyes. The acetylation of the silane bridge to change the total charge of the supports produced contrasting results; Oxone is as expected a better oxidant than hydrogen peroxide. On the other hand, it is rather expensive and is not so 'green' in comparison to hydrogen peroxide, which produces water only as the product of the oxidation reactions. Further work is in progress to better understand the behavior of the studied catalysts and to find new applications.

The homogeneous catalyst (MnTDCPP)Cl has been studied with promising results. Several products were formed after a disappearance of the 100% of the original substrate (Bifonazole). Future work is in progress in order to to fully assess and identify the products pattern, and to include more antimycotic drugs.

These preliminary results show that biomimetic metalloporphyrins are an effective alternative for the removal of antimycotic drugs under mild operational conditions. Besides, this catalytic system, emulating enzymatic activity of cytochrome P450, could help to

better understand the metabolism of drugs and their metabolites being released in the environment.

5 Bibliography

1. Zucca, P., et al., *Biomimetic metalloporphines and metalloporphyrins as potential tools for delignification: Molecular mechanisms and application perspectives.* Journal of Molecular Catalysis A: Chemical, 2014. **388–389**: p. 2-34.
2. Zucca, P., et al., *Degradation of textile dyes using immobilized lignin peroxidase-like metalloporphines under mild experimental conditions.* Chemistry Central Journal, 2012. **6**(1): p. 1-8.
3. Zhou, X., et al., *Evidence of Two Key Intermediates Contributing to the Selectivity of P450-Biomimetic Oxidation of Sulfides to Sulfoxides and Sulfones.* Chemistry – An Asian Journal, 2012. **7**(10): p. 2253-2257.
4. Zucca, P., A. Rescigno, and E. Sanjust, *Ligninolytic peroxidase-like activity of a synthetic metalloporphine immobilized onto mercapto-grafted crosslinked PVA inspired by the active site of cytochrome P450.* Chin J Catal, 2011. **32**.
5. Zucca, P., et al., *Degradation of Alizarin Red S under mild experimental conditions by immobilized 5,10,15,20-tetrakis(4-sulfonatophenyl)porphine-Mn(III) as a biomimetic peroxidase-like catalyst.* Journal of Molecular Catalysis A: Chemical, 2008. **288**(1-2): p. 97-102.
6. Zucca, P., et al., *Fe(III)-5,10,15,20-Tetrakis(pentafluorophenyl)porphine supported on pyridyl-functionalized, crosslinked poly(vinylalcohol) as a biomimetic versatile-peroxidase-like catalyst.* J Mol Catal A Chem, 2009. **306**.
7. Smith, A.T. and N.C. Veitch, *Substrate binding and catalysis in heme peroxidases.* Current Opinion in Chemical Biology, 1998. **2**(2): p. 269-278.
8. Welinder, K.G., *Superfamily of plant, fungal and bacterial peroxidases.* Current Opinion in Structural Biology, 1992. **2**(3): p. 388-393.
9. Poulos, T.L., et al., *CRYSTALLOGRAPHIC REFINEMENT OF LIGNIN PEROXIDASE AT 2-ANGSTROM.* Journal of Biological Chemistry, 1993. **268**(6): p. 4429-4440.
10. Nagano, S., et al., *Putative hydrogen bond network in the heme distal site of horseradish peroxidase.* Biochemical and Biophysical Research Communications, 1995. **207**(1): p. 417-423.
11. Rebelo, S.L.H., et al., *Mechanistic studies on metalloporphyrin epoxidation reactions with hydrogen peroxide: Evidence for two active oxidative species.* Journal of Catalysis, 2005. **234**(1): p. 76-87.
12. Fertinger, C., A. Franke, and R. van Eldik, *Mechanistic insight from thermal activation parameters for oxygenation reactions of different substrates with biomimetic iron porphyrin models for compounds I and II.* J Biol Inorg Chem, 2012. **17**(1): p. 27-36.
13. De Visser, S.P., J.S. Valentine, and W. Nam, *A biomimetic ferric hydroperoxo porphyrin intermediate.* Angewandte Chemie - International Edition, 2010. **49**(12): p. 2099-2101.
14. Harris, D.L., *High-valent intermediates of heme proteins and model compounds.* Curr Opin Chem Biol, 2001. **5**(6): p. 724-35.
15. Everse, J., *The structure of heme proteins compounds I and II: Some misconceptions.* Free Radical Biology and Medicine, 1998. **24**(7-8): p. 1338-1346.
16. Silaghi-Dumitrescu, R., *The nature of the high-valent complexes in the catalytic cycles of hemoproteins.* Journal of Biological Inorganic Chemistry, 2004. **9**(4): p. 471-476.

17. Green, M.T., *Application of Badger's rule to heme and non-heme iron-oxygen bonds: An examination of ferryl protonation states.* Journal of the American Chemical Society, 2006. **128**(6): p. 1902-1906.
18. Saritha, M., A. Arora, and L. Nain, *Pretreatment of paddy straw with Trametes hirsuta for improved enzymatic saccharification.* Bioresource Technology, 2012. **104**: p. 459-465.
19. Pakshirajan, K., S. Jaiswal, and R.K. Das, *Biodecolourization of azo dyes using Phanerochaete chrysosporium: Effect of culture conditions and enzyme activities.* Journal of scientific and industrial research, 2011. **70**(11): p. 987-991.
20. Mirzaakhmedov, S.Y., et al., *Isolation and purification of lignoperoxidase from the mushroom Pleurotus ostreatus.* Chemistry of Natural Compounds, 2007. **43**(6): p. 682-684.
21. Vahabzadeh, F., A. Mogharei, and M. Mehranian, *Decolorization of molasses waste water from an alcoholic fermentation process with Phanerochaete chrysosporium - Involvement of ligninase.* Iranian Journal of Chemistry and Chemical Engineering, 2002. **21**(2): p. 126-134.
22. Fu, J., et al., *Bio-processing of bamboo fibres for textile applications: A mini review.* Biocatalysis and Biotransformation, 2012. **30**(1): p. 141-153.
23. Doyle, W.A., et al., *Two substrate interaction sites in lignin peroxidase revealed by site- directed mutagenesis.* Biochemistry, 1998. **37**(43): p. 15097-15105.
24. Mylrajan, M., et al., *Resonance Raman spectroscopic characterization of compound III of lignin peroxidase.* Biochemistry, 1990. **29**(41): p. 9617-9623.
25. Wariishi, H. and M.H. Gold, *Lignin peroxidase compound III. Mechanism of formation and decomposition.* Journal of Biological Chemistry, 1990. **265**(4): p. 2070-2077.
26. Hammel, K.E., B. Kalyanaraman, and T.K. Kirk, *Substrate free radicals are intermediates in ligninase catalysis.* Proceedings of the National Academy of Sciences of the United States of America, 1986. **83**(11): p. 3708-3712.
27. Hammel, K.E. and D. Cullen, *Role of fungal peroxidases in biological ligninolysis.* Current Opinion in Plant Biology, 2008. **11**: p. 349-355.
28. Hammel, K.E., et al., *Ligninolysis by a purified lignin peroxidase.* Journal of Biological Chemistry, 1993. **268**(17): p. 12274-12281.
29. Piontek, K., A.T. Smith, and W. Blodig, *Lignin peroxidase structure and function.* Biochemical Society Transactions, 2001. **29**(2): p. 111-116.
30. Hofrichter, M., *Review: Lignin conversion by manganese peroxidase (MnP).* Enzyme and Microbial Technology, 2002. **30**(4): p. 454-466.
31. Kishi, K., et al., *Mechanism of manganese peroxidase compound II reduction. Effect of organic acid chelators and pH.* Biochemistry, 1994. **33**(29): p. 8694-8701.
32. Wariishi, H., L. Akileswaran, and M.H. Gold, *Manganese peroxidase from the basidiomycete Phanerochaete chrysosporium: Spectral characterization of the oxidized states and the catalytic cycle.* Biochemistry, 1988. **27**(14): p. 5365-5370.
33. Camarero, S., et al., *Description of a versatile peroxidase involved in the natural degradation of lignin that has both manganese peroxidase and lignin peroxidase substrate interaction sites.* Journal of Biological Chemistry, 1999. **274**(15): p. 10324-10330.
34. Dau, H.A., et al., *The coprophilous mushroom Coprinus radians secretes a haloperoxidase that catalyzes aromatic peroxygenation.* Applied and Environmental Microbiology, 2007. **73**(17): p. 5477-5485.

35. Kinne, M., et al., *Stepwise oxygenations of toluene and 4-nitrotoluene by a fungal peroxygenase.* Biochemical and Biophysical Research Communications, 2010. **397**(1): p. 18-21.
36. Ullrich, R., et al., *Pyridine as novel substrate for regioselective oxygenation with aromatic peroxygenase from Agrocybe aegerita.* FEBS Letters, 2008. **582**(29): p. 4100-4106.
37. Ullrich, R., et al., *Novel haloperoxidase from the agaric basidiomycete Agrocybe aegerita oxidizes aryl alcohols and aldehydes.* Applied and Environmental Microbiology, 2004. **70**(8): p. 4575-4581.
38. Hofrichter, M., et al., *New and classic families of secreted fungal heme peroxidases.* Appl Microbiol Biotechnol, 2010. **87**(3): p. 871-97.
39. Yarman, A., et al., *The aromatic peroxygenase from Marasmius rutola--a new enzyme for biosensor applications.* Anal Bioanal Chem, 2012. **402**(1): p. 405-12.
40. Berezin, B.D., *Some peculiarities of the molecular structure of porphine and its complexes.* Chemistry of Heterocyclic Compounds. **1**(6): p. 641-643.
41. Walker, F.A. and U. Simonis, *Proton NMR Spectroscopy of Model Hemes*, in *NMR of Paramagnetic Molecules*, L.J. Berliner and J. Reuben, Editors. 1993, Springer US: Boston, MA. p. 133-274.
42. Dolphin, D., T.G. Traylor, and L.Y. Xie, *Polyhaloporphyrins: Unusual Ligands for Metals and Metal-Catalyzed Oxidations.* Accounts of Chemical Research, 1997. **30**(6): p. 251-259.
43. Goh, Y.M. and W. Nam, *Significant electronic effect of porphyrin ligand on the reactivities of high-valent iron(IV) oxo porphyrin cation radical complexes.* Inorganic Chemistry, 1999. **38**(5): p. 914-920.
44. Jin, N. and J.T. Groves, *Unusual kinetic stability of a ground-state singlet oxomanganese(V) porphyrin. Evidence for a spin state crossing effect.* Journal of the American Chemical Society, 1999. **121**(12): p. 2923-2924.
45. Tsuchiya, S. and M. Seno, *Novel Synthetic Method of Phenol from Benzene Catalysed by Perfluorinated Hemin.* Chemistry Letters, 1989. **18**(2): p. 263-266.
46. Kadish, K.M., et al., *Syntheses and spectroscopic characterization of (T(P-Me2N)F4PP)H2 and (7(p-Me2N)F4PP)M where 7(p-Me2N)F4PP is the dianion of meso-tetrakis(o,o,w,w-tetrafluoro-p-(dimethylamino)phenyl)-porphyrin and M = Co(II), Cu(II), or Ni(II).* Journal of the American Chemical Society, 1990. **112**(23): p. 8364-8368.
47. Zipplies, M.F., W.A. Lee, and T.C. Bruice, *Influence of hydrogen ion activity and general acid-base catalysis on the rate of decomposition of hydrogen peroxide by a novel nonaggregating water-soluble iron(III) tetraphenylporphyrin derivative.* Journal of the American Chemical Society, 1986. **108**(15): p. 4433-4445.
48. Almarsson, Ö., H. Adalsteinsson, and T.C. Bruice, *Synthesis and characterization of an octacationic iron(III) tetraphenylporphyrin, which Is soluble in water and N non-μ-oxo dimer forming.* Journal of the American Chemical Society, 1995. **117**(16): p. 4524-4532.
49. Mansuy, D., *A brief history of the contribution of metallporphyrin models to cytochrome P450 chemistry and oxidation catalysis.* C. R. Chimie, 2007. **10**: p. 392-413.
50. Rocha-Gonsalves, A.M.A. and M.M. Pereira, *State of the art in the development of biomimetic oxidation catalysts.* Journal of Molecular Catalysis A: Chemical, 1996. **113**: p. 209-221.
51. McLain, J.L., J. Lee, and J.T. Groves, *Biomimetic Oxygenations Related to Cytochrome P450: Metal-Oxo and Metal-Peroxo Intermediates*, in *Biomimentic*

Oxidations Catalyzed by Transition Metal Complexes, B. Meunier, Editor. 2000, Imperial College Press: London. p. 91-170.
52. De Montellano, P.R.O., *Control of the catalytic activity of prosthetic heme by the structure of hemoproteins.* Accounts of Chemical Research, 1987. **20**(8): p. 289-294.
53. Meunier, B., S.P. de Visser, and S. Shaik, *Mechanism of oxidation reactions catalyzed by cytochrome P450 enzymes.* Chemical Reviews, 2004. **104**(9): p. 3947-3980.
54. Hrycay, E.G. and S.M. Bandiera, *The monooxygenase, peroxidase, and peroxygenase properties of cytochrome P450.* Arch Biochem Biophys, 2012. **522**(2): p. 71-89.
55. Meunier, B., *Metalloporphyrins as versatile catalysts for hydrocarbon oxygenations and oxidative DNA cleavage.* Chemical Reviews, 1992. **92**: p. 1411-1456.
56. Groves, J.T. and Y.-Z. Han, *Models and Mechanisms of Cytochrome P450 Action*, in *Cytochrome P450: Structure, Mechanism, and Biochemistry*, P.R.O. De Montellano, Editor. 1995, Plenum Press: New York.
57. Rohmer, M.-M., A. Strich, and A. Veillard, *Conformational preferences of the axial ligands in some metalloporphyrins. A theoretical study.* Theoretica chimica acta. **65**(3): p. 219-231.
58. Zucca, P., et al., *Fe(III)-5,10,15,20-Tetrakis(pentafluorophenyl)porphine supported on pyridyl-functionalized, crosslinked poly(vinylalcohol) as a biomimetic versatile-peroxidase-like catalyst.* Journal of Molecular Catalysis A: Chemical, 2009. **306**(1-2): p. 89-96.
59. *Silica Fume User's Manual.* Silica Fume Association, 2005.
60. Cruz, J.C., P.H. Pfromm, and M.E. Rezac, *Immobilization of Candida antarctica Lipase B on fumed silica.* Process Biochemistry, 2009. **44**(1): p. 62-69.
61. Cruz, J.C., et al., *Conformational changes and catalytic competency of hydrolases adsorbing on fumed silica nanoparticles: I. Tertiary structure.* Colloids and Surfaces B: Biointerfaces, 2010. **79**(1): p. 97-104.
62. Cruz, J.C., et al., *Conformational changes and catalytic competency of hydrolases adsorbing on fumed silica nanoparticles: II. Secondary structure.* Colloids and Surfaces B: Biointerfaces, 2010. **81**(1): p. 1-10.
63. Gun'ko, V.M., et al., *Aqueous Suspensions of Fumed Silica and Adsorption of Proteins.* Journal of Colloid and Interface Science, 1997. **192**(1): p. 166-178.
64. Langhals, H., *Color Chemistry. Synthesis, Properties and Applications of Organic Dyes and Pigments. 3rd revised edition. By Heinrich Zollinger.* Angewandte Chemie International Edition, 2004. **43**(40): p. 5291-5292.
65. Platzek, T., et al., *Formation of a carcinogenic aromatic amine from an azo dye by human skin bacteria in vitro.* Hum Exp Toxicol, 1999. **18**(9): p. 552-9.
66. Walthall, W.K. and J.D. Stark, *The acute and chronic toxicity of two xanthene dyes, fluorescein sodium salt and phloxine B, to Daphnia pulex.* Environmental Pollution, 1999. **104**(2): p. 207-215.
67. Carliell C.M., B.S.J., Naidoo N., Buckley C.A., Mulholland D.A., Senior E. , *Anaerobic decolourisation of reactive dyes in conventional sewage treatment processes. Water S.A.* 2004.
68. Vandevivere, P.C., R. Bianchi, and W. Verstraete, *Review: Treatment and reuse of wastewater from the textile wet-processing industry: Review of emerging technologies.* Journal of Chemical Technology & Biotechnology, 1998. **72**(4): p. 289-302.

69. Robinson, T., et al., *Remediation of dyes in textile effluent: a critical review on current treatment technologies with a proposed alternative.* Bioresource Technology, 2001. **77**(3): p. 247-255.
70. Carliell C.M., B.S.J., Buckley C.A., *Treatment of exhausted reactive dye bath effluent using anaerobic digestion: laboratory and full scale trials. Water S.A.* 1996.
71. Rai, H.S., Bhattacharyya M.S., Singh J., Bansal T.K., Vats P., Banerjee U.C. , *Removal of dyes from the effluent of textile and dyestuff manufacturing industry. A review of emerging techniques with reference to biological treatment.* 2005.
72. Ţurcaş, C.V. and I. Sebe, *Azo dyes complexes. Synthesis and tinctorial properties.* UPB Scientific Bulletin, Series B: Chemistry and Materials Science, 2012. **74**(1): p. 109-118.
73. *The Society of Dyers and Colourists, Bradford,UK.* Colour Index, 3rd Edition, 1971. **Vol. 4**.
74. Mujumdar, R.B., et al., *Cyanine dye labeling reagents: Sulfoindocyanine succinimidyl esters.* Bioconjugate Chemistry, 1993. **4**(2): p. 105-111.
75. Pardal, A.C., et al., *Synthesis and fixation of aminocyanines to microcrystalline cellulose using cyanuric chloride as a cross-linking agent.* Coloration Technology, 2001. **117**(1): p. 43-48.
76. Zollinger, H., *Color Chemistry: Syntheses, Properties, and Applications of Organic Dyes and Pigments*. 2003: Wiley.
77. Fabian, J., *Colour and constitution of organic molecules. J. Griffiths, 1. Aufl., 281 S., 53 Abb., 29 Tab., Academic Press, London/New York/San Francisco 1976. geb., 9, 50£.* Journal für Praktische Chemie, 1978. **320**(5): p. 878-879.
78. Clifton, J., 2nd and J.B. Leikin, *Methylene blue.* Am J Ther, 2003. **10**(4): p. 289-91.
79. Chou, C.H.S.J., S. United, and C. Syracuse Research, *Toxicological profile for hydrogen sulfide*. Toxicological profile for hydrogen sulfide (update). 2006, [Atlanta, Ga.]: U.S. Dept. of Health and Human Services, Public Health Service, Agency for Toxic Substances and Disease Registry. xx, 208, [24] p.
80. Ghosh, T.K. and E.L. Tollefson, *KINETIC AND REACTION MECHANISM OF HYDROGEN SULFIDE OXIDATION OVER ACTIVATED CARBON IN THE TEMPERATURE RANGE OF 125-200 degree C.* Canadian Journal of Chemical Engineering, 1986. **64**(6): p. 969-976.
81. Ma, Y., J. Zhao, and B. Yang, *Removal of H2S in waste gases by an activated carbon bioreactor.* International Biodeterioration and Biodegradation, 2006. **57**(2): p. 93-98.
82. Makaruk, A., M. Miltner, and M. Harasek, *Biogas desulfurization and biogas upgrading using a hybrid membrane system ,ãØ Modeling study.* Water Science and Technology, 2013. **67**(2): p. 326-332.
83. Liu, C., et al., *Removal of H2S by co-immobilized bacteria and fungi biocatalysts in a bio-trickling filter.* Process Safety and Environmental Protection, 2013. **91**(1-2): p. 145-152.
84. Zhou, X., et al. *Biomimetic oxidation of sulfides based on Fe III porphyrin under the mild conditions*. 2012.
85. Oldfield, C., et al., *Elucidation of the metabolic pathway for dibenzothiophene desulphurization by Rhodococcus sp. strain IGTS8 (ATCC 53968).* Microbiology, 1997. **143 (Pt 9)**: p. 2961-73.
86. Ohshiro, T., T. Hirata, and Y. Izumi, *Microbial desulfurization of dibenzothiophene in the presence of hydrocarbon.* Applied Microbiology and Biotechnology, 1995. **44**(1-2): p. 249-252.

87. Negishi, O. and T. Ozawa, *Effect of Polyphenol Oxidase on Deodorization.* Bioscience, Biotechnology and Biochemistry, 1997. **61**(12): p. 2080-2084.
88. Fengel D and Wegener G. Wood, B., *Chemistry, Ultrastructure, Reactions. Walter de*

Gruyte , Berlin. 1989.
89. Higuchi, T., *Lignin biochemistry: Biosynthesis and biodegradation.* Wood Science and Technology. **24**(1): p. 23-63.
90. Dittmar, T. and R.J. Lara, *Molecular evidence for lignin degradation in sulfate-reducing mangrove sediments (Amazônia, Brazil).* Geochimica et Cosmochimica Acta, 2001. **65**(9): p. 1417-1428.
91. Goujon, T., et al., *Genes involved in the biosynthesis of lignin precursors in Arabidopsis thaliana.* Plant Physiology and Biochemistry, 2003. **41**(8): p. 677-687.
92. Kögel-Knabner, I., *The macromolecular organic composition of plant and microbial residues as inputs to soil organic matter.* Soil Biology and Biochemistry, 2002. **34**(2): p. 139-162.
93. Tien, M. and K. Kirk, *Lignin-degrading enzyme from Phanerochaete chrysosporium: purification, characterization, and catalytic properties of a unique H_2O_2-requiring oxygenase.* Proceedings of the National Academy of Sciences, USA, 1984. **81**: p. 2280-2284.
94. Guarner, J. and M.E. Brandt, *Histopathologic Diagnosis of Fungal Infections in the 21st Century.* Clinical Microbiology Reviews, 2011. **24**(2): p. 247-280.
95. Hamill, R.J., *Amphotericin B Formulations: A Comparative Review of Efficacy and Toxicity.* Drugs, 2013. **73**(9): p. 919-934.
96. Tafi, A., et al., *Azole Fungicides. Comfa Study of Candida Albicans Lanosterol 14α-Demethylase Azole Inhibitors*, in *Spectroscopy of Biological Molecules: 6th European Conference on the Spectroscopy of Biological Molecules, 3–8 September 1995, Villeneuve d'Ascq, France*, J.C. Merlin, S. Turrell, and J.P. Huvenne, Editors. 1995, Springer Netherlands: Dordrecht. p. 157-158.
97. Zucca, P., et al., *Fe(III)-5,10,15,20-tetrakis(pentafluorophenyl)porphine supported on pyridyl-functionalized, crosslinked poly(vinyl alcohol) as a biomimetic versatile-peroxidase-like catalyst.* Journal of Molecular Catalysis A: Chemical, 2009. **306**(1-2): p. 89-96.
98. Cano-Serrano, E., J.M. Campos-Martin, and J.L.G. Fierro, *Sulfonic acid-functionalized silica through quantitative oxidation of thiol groups.* Chemical Communications, 2003(2): p. 246-247.
99. M. Kirihara, A.I., T. Noguchi, and J. Yamamoto, , *"Tantalum carbide or niobium carbide catalyzed oxidation of sulfides with hydrogen peroxide: Highly efficient and chemoselective syntheses of sulfoxides and sulfones,.* Synlett, no. 10, 2010.

100. Baciocchi, E., M.F. Gerini, and A. Lapi, *Synthesis of sulfoxides by the hydrogen peroxide induced oxidation of sulfides catalyzed by iron tetrakis(pentafluorophenyl)porphyrin: Scope and chemoselectivity.* Journal of Organic Chemistry, 2004. **69**(10): p. 3586-3589.
101. Moghadam, M., et al., *Biomimetic oxidation of sulfides with sodium periodate catalyzed by polystyrene-bound manganese (III) tetrapyridylporphyrin.* Applied Catalysis A: General, 2008. **349**(1–2): p. 177-181.
102. Ghaemi, A., et al., *Highly efficient oxidation of sulfides to sulfones with tetra-n-butylammonium hydrogen monopersulfate catalyzed by β-tri- and tetra-brominated meso-tetraphenylporphyrinatomanganese(III) acetate.* Applied Catalysis A: General, 2009. **353**(2): p. 154-159.

103. Rezaeifard, A., et al., *Factors affecting the reactivity and selectivity in the oxidation of sulfides with tetra-n-butylammonium peroxomonosulfate catalyzed by Mn(III) porphyrins: Significant nitrogen donor effects.* Polyhedron, 2011. **30**(4): p. 592-598.
104. H. B. Dunford, *Heme Peroxidase, JohnWiley & Sons,New York, NY, USA,*. 1999.
105. Baciocchi, E., et al., *Mechanism of the oxidation of aromatic sulfides catalysed by a water soluble iron porphyrin.* Organic and Biomolecular Chemistry, 2003. **1**(2): p. 422-426.
106. Goto, Y., et al., *Mechanisms of Sulfoxidation Catalyzed by High-Valent Intermediates of Heme Enzymes: Electron-Transfer vs Oxygen-Transfer Mechanism.* Journal of the American Chemical Society, 1999. **121**(41): p. 9497-9502.
107. Baciocchi, E., et al., *Oxidation of Sulfides by Peroxidases. Involvement of Radical Cations and the Rate of the Oxygen Rebound Step.* Journal of the American Chemical Society, 1996. **118**(37): p. 8973-8974.
108. Ando, W., R. Tajima, and T. Takata, *Oxidation of sulfide with ArIO catalyzed with TPPM(III)Cl.* Tetrahedron Letters, 1982. **23**(16): p. 1685-1688.
109. Zucca, P., et al., *5,10,15,20-Tetrakis(4-sulfonato-phenyl)porphine-Mn(III) immobilized on imidazole activacted silica as a novel lignin-peroxidase-like biomimetic catalyst.* Journal of Molecular Catalysis A: Chemical, 2007. **278**(1-2): p. 220-227.
110. Archibald, F.S., *A new assay for lignin-type peroxidases employing the dye Azure B.* Applied and Environment Microbiology, 1992. **58**(9): p. 3110-3116.
111. Zucca, P., et al., *Is the bleaching of phenosafranine by hydrogen peroxide oxidation catalyzed by silica-supported 5,10,15,20-tetrakis-(sulfonatophenyl)porphine-Mn(III) really biomimetic?* Journal of Molecular Catalysis A: Chemical, 2010. **321**: p. 27-33.
112. Zucca, P., A. Rescigno, and E. Sanjust, *Ligninolytic peroxidase-like activity of a synthetic metalloporphine immobilized onto mercapto-grafted crosslinked PVA inspired by the active site of cytochrome P450.* Chinese Journal of Catalysis, 2011. **32**(11): p. 1663-1666.
113. Agarwala, A. and D. Bandyopadhyay, *Cytochrome P-450 model compound catalyzed selective hydroxylation of C–H bonds: Dramatic solvent effect.* Chemical Communications (Cambridge), 2006: p. 4823-4825.
114. Zucca, P., et al., *Induction, purification, and characterization of a laccase isozyme from Pleurotus sajor-caju and the potential in decolorization of textile dyes.* Journal of Molecular Catalysis B: Enzymatic, 2011. **68**(2): p. 216-222.
115. Kosman, D.J., *Multicopper oxidases: a workshop on copper coordination chemistry, electron transfer, and metallophysiology.* JBIC Journal of Biological Inorganic Chemistry, 2009. **15**(1): p. 15-28.
116. Huang, H., G. Zoppellaro, and T. Sakurai, *Spectroscopic and kinetic studies on the oxygen-centered radical formed during the four-electron reduction process of dioxygen by Rhus vernicifera laccase.* J Biol Chem, 1999. **274**(46): p. 32718-24.
117. van Rantwijk, F. and R.A. Sheldon, *Selective oxygen transfer catalysed by heme peroxidases: synthetic and mechanistic aspects.* Current Opinion in Biotechnology, 2000. **11**(6): p. 554-564.
118. Doerge, D.R., N.M. Cooray, and M.E. Brewster, *Peroxidase-catalyzed S-oxygenation: mechanism of oxygen transfer for lactoperoxidase.* Biochemistry, 1991. **30**(37): p. 8960-8964.

119. Mansuy, D., *A brief history of the contribution of metalloporphyrin models to cytochrome P450 chemistry and oxidation catalysis.* Comptes Rendus Chimie, 2007. **10**(4–5): p. 392-413.
120. Groves, J.T., *Reactivity and mechanisms of metalloporphyrin-catalyzed oxidations.* Journal of Porphyrins and Phthalocyanines, 2000. **04**(04): p. 350-352.
121. Haemmerli, S.D., et al., *Oxidation of veratryl alcohol by the lignin peroxidase of Phanerochaete chrysosporium Involvement of activated oxygen.* FEBS Letters, 1987. **220**(1): p. 149-154.
122. Fukushima, M., *Oxidative degradation of pentachlorophenol by an iron(III)-porphyrin catalyst bound to humic acid via formaldehyde polycondensation.* Journal of Molecular Catalysis A: Chemical, 2008. **286**(1-2): p. 47-54.
123. Fukushima, M., S. Shigematsu, and S. Nagao, *Influence of humic acid type on the oxidation products of pentachlorophenol using hybrid catalysts prepared by introducing iron(III)-5,10,15,20-tetrakis(p-hydroxyphenyl) porphyrin into hydroquinone-derived humic acids.* Chemosphere, 2010. **78**(9): p. 1155-1159.
124. Zucca P., S.M.Q., Neves M. G. P. M. S. , Cocco G. ,Sanjust E., *Immobilized lignin peroxidase-like metalloporphines as reusable catalysts in industrial dye oxidative bleaching.* Molecules, 2015.
125. Neves, C.M.B., et al., *Oxidation of diclofenac catalyzed by manganese porphyrins: synthesis of novel diclofenac derivatives.* RSC Advances, 2012. **2**(19): p. 7427-7438.